



IGC Newsletter

IN THIS ISSUE

Interaction with Eminent Colleagues

- Interaction with Dr. Srikumar Banerjee

Technical Articles

- Utilisation of Shake Table Facilities at the Structural Mechanics Laboratory
- Impression Creep: An Innovative Testing Technique for Evaluation of Creep Properties of Materials

Young Officer's Forum

- Investigation of Structural and Optical Properties of ECR-CVD Grown Ultra Smooth DLC Films

Young Researcher's Forum

- Thermodynamics and Kinetics of Phase Transformation in Ti-Ta-Nb Alloy

Conference / Meeting Highlights

- Technology Day Celebrations 2013

News and Events

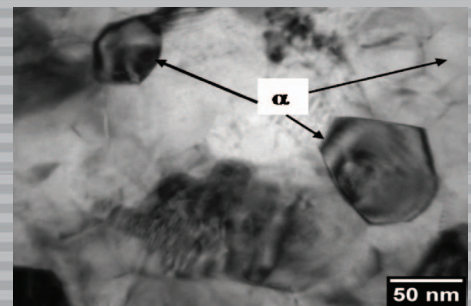
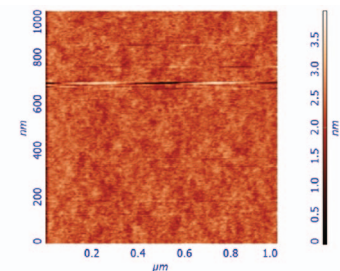
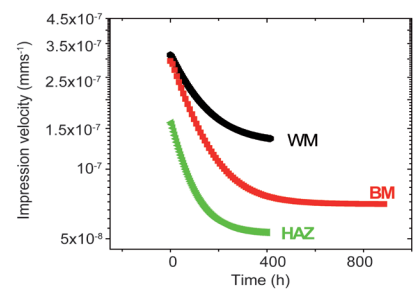
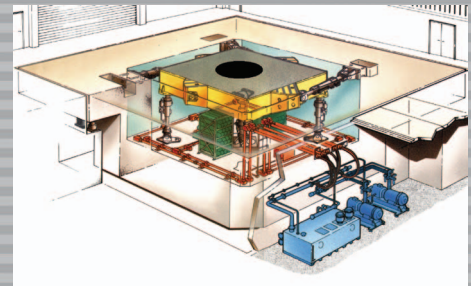
- Safety Promotional Activities

Forthcoming Meeting/Conference

- International Conference on Structural Integrity (ICONS)

Visit of Dignitaries

Awards & Honours



From the Editor

Dear Reader

It is my pleasant privilege to forward a copy of the latest issue of IGC Newsletter (Volume 97, July 2013 issue).

We have continued with the new feature in the Newsletter, the interview of an eminent person by a team of young officers. In this issue we have had the privilege of Dr. Srikumar Banerjee, DAE Homi Bhabha Chair Professor & Former Chairman, AEC, sharing his experiences with young colleagues of the Centre.

In the first technical article Dr. P. Chellapandi and colleagues depict the utilisation of shake table facilities at the Structural Mechanics Laboratory, which have been extensively used for various seismic qualifications tests.

In the second technical article, Dr. M. D. Mathew and colleagues have described an innovative testing technique and development of a unique Impression Creep Testing Facility for evaluating the creep properties of materials such as 316LN SS.

In the Young Officer's forum, Shri Syamala Rao Polaki has investigated the structural and optical properties of electron cyclotron resonance plasma chemical vapor deposition (ECR-CVD) grown ultra smooth diamond like carbon films.

Dr. Madhusmita Behera has described the thermodynamics and kinetics of $\alpha \leftrightarrow \beta$ phase transformation in Ti-Ta-Nb alloy, in the Young Researcher's Forum.

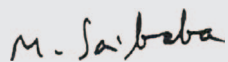
This Newsletter carries reports on the "Technology Day Celebrations 2013" and "Safety Promotional Activities".

A delegation of Editors/Senior Journalists from Nepal, Dr. Jatinder V. Yakhmi, Chairman, Atomic Energy Education Society, Mumbai, Dr. Srikumar Banerjee, DAE Homi Bhabha Chair Professor & Former Chairman, AEC visited the Centre during the last quarter.

We are happy to share with you the awards, honours and distinctions earned by our colleagues.

We look forward to your comments, continued guidance and support.

With my best wishes and personal regards



(M. Sai Baba)

Chairman, Editorial Committee, IGC Newsletter

&

Associate Director, Resources Management Group

Interaction with Dr. Srikumar Banerjee



Dr. Srikumar Banerjee interacting with the team of young officers and Dr. M. Sai Baba, AD, RMG

Sir, we all know about Dr. Srikumar Banerjee the professional, please tell us something about Srikumar Banerjee the person What are your hobbies, How do you spend your spare time?

Truly speaking I could never develop a hobby seriously due to lack of time. I enjoyed reading outside my subject, particularly literature. I am not a voracious reader, but I have read Bengali literature during my young age and what I have read during that time is still imprinted in my mind. I also enjoyed taking part in outdoor sports in my student days. Reading now is more sporadic in nature, due to various commitments. I like listening to music, particularly Tagore songs. As a researcher, if you want to make a mark in your career, 24 hours are not enough. You have to apply yourself fully. In DAE, one also needs to work towards mission oriented activities, achieve goals within a specific time limit. For this, you have to interact with people from multidisciplinary background, learn about the work they do, other than your own research. Without this knowledge, the larger picture cannot be seen and you cannot take up greater responsibilities in the Department. I have done some teaching in Training School and I enjoyed it. In short I cannot say that I have a specific hobby. A little spare time that I get, I like it to spend with my family.

Why did you take up metallurgy in your undergraduation?

Frankly speaking, I was not interested in Engineering and more inclined to Physics. Also I had some apprehension for leaving my home and moving to a hostel for studying Engineering. My father advised me "whether you take up the course at IIT or not, just appear for the exam and gain experience". In those days, a book containing question papers of the last ten years was available in the market and my father bought me



Dr. Srikumar Banerjee is a DAE Homi Bhabha Chair Professor in Bhabha Atomic Research Centre (BARC), Mumbai and first Chancellor of the Central University of Kashmir (CUK). He is a former Chairman of Atomic Energy Commission and Secretary to the Government of India, Department of Atomic Energy. He joined BARC in 1967 after obtaining B. Tech. in Metallurgical Engineering from Indian Institute of Technology (IIT), Kharagpur. He also obtained Ph.D in Metallurgical Engineering from IIT, Kharagpur. As a Director of BARC during 2004-2010, he provided leadership in the development of Advanced Reactor Technology, Fuel Cycle technology and strategic programmes. He is one of the leading experts in Materials Science and Technology and made outstanding contributions to many materials related areas. His comprehensive work on physical metallurgy of zirconium alloys and radiation induced order-disorder transition in alloys are widely quoted in scientific literature. His work has also provided a basis for developing a novel fabrication schedule for the pressure tubes used in the Indian Pressurised Heavy Water Reactors (PHWRs). He is a recipient of 'Shanti Swarup Bhatnagar Award in Engineering Sciences' in 1989, 'Indian National Science Academy (INSA) Award for Materials Science' in 2001, Padma Shri from Govt. of India (a Civilian honour - 2005), 'Indian Science Congress Association's Excellence in Science and Technology Award' in 2010. Notable among the international awards are 'Acta Metallurgica Outstanding Paper Award' in 1984 and 'Alexander von Humboldt Research Award' in 2004 and ASTM William J. Kroll Zirconium Medal in 2013.

one to prepare for the entrance exam. While choosing the discipline, to fill the IIT application, I opted for Metallurgy due to the boom in the steel industry at that point of time and my second choice was Electronics. The other reason for me to take up Metallurgy was that, it offered a bridge between engineering and basic science disciplines. I was more inclined towards Physics than Chemistry in those days. My giving Metallurgy and Electronics as higher choices over Mechanical Engineering (which used to be generally the first choice) was because I felt that Metallurgy and Electronics were more Physics based. I remember that I once asked Prof. P.R. Dhar, Head, Metallurgy Department at IIT, Kharagpur during the first year 'Introduction to Metallurgy' course, why should we read so much about physical optics. At that time I had no idea that during major part of my research career I would be working on Electron Microscopy which is essentially based on the concepts of physical optics.

When I was inducted in a research group, initially I had to grow a taste for research – which I believe is possible only through interactions with your seniors. I was very lucky in that respect to have Dr. R. Krishnan, Dr. M.K. Asundi, Dr. V.S. Arunachalam, Dr. B.D. Sharma, Dr. C.K. Gupta and Dr. P. Mukhopandhyay as my senior colleagues in Metallurgy Division, who all have moulded my attitude towards research. Once one grows that taste, advancing in one's research career becomes relatively easy in spite of many obstacles which come on the way. A stage comes when you start enjoying your work. As you go further you see the connection between your work and the broader objectives of the Department. That is how one gets inducted into the system and get a direction for expressing one's creativity in a manner that contributes to the overall programme.

Do you believe in role models? Who was your role model?

I believe that each one of us must have role models not only of someone of whom we have read but also from those who are present in flesh and blood before us. Obviously, some teachers leave a deep impression on you. I was fortunate enough to have many such people before me. Dr. Chandrashekar in Thermodynamics, Dr. Trasi in Mathematics, Dr. L.V. Krishnan in Reactor Physics were some of our teachers who had given deep insights into these subjects. Dr. R. Chidambaram started taking the classes in Statistical Thermodynamics complementing Shri C.V. Sundaram's course on Chemical Thermodynamics in the 12th Batch. Though I was from the 11th Batch, I used to attend those classes. Both of them were not only very good teachers, as fine human beings they had deep influence on me. Dr. G. Venkatraman who started the Physics programme at IGCAR used to lecture on topics in Condensed Matter Physics and Phase Transitions. These lectures had big impacts on my work at a later date. In 1971 I got an opportunity to attend a Summer School in Banaras Hindu University where I met some stalwarts including Prof. Anantharaman, Prof. Ramarao, Prof. Lele and Prof. Ranganathan who made a lasting impact in my research career.

What was your motivation for joining DAE?

I did not aspire to join DAE but it just happened. Actually in those days, not many from IITs were applying for BARC Training School. Someone told me about the advertisement for admission to BARC Training School and I applied. I boarded a newly started AC Chair Car train from Kolkata to Mumbai to attend the interview and met a number of applicants travelling by the same train. I made a few friends during the journey and seeing their keenness and competitive spirit I got enthused to join DAE. The day I was interviewed, it was raining heavily and I remember draining my shoes inside out after entering the interview premises. Interview was good. The questions asked were intelligent and subject relevant. That is how it all started for me.

In the final year of my undergraduate course, there was a subject on 'Nuclear Materials' and the reference book was by Glasstone and Sesonske, which had a cover page photograph showing a nuclear reactor surrounded by greenery, hills and the sea. I thought it would be wonderful if I can get an opportunity to work in an environment like that. When I entered the Trombay Campus which has a forest covered hill on one side and the sea on the other, I really felt that my dream was fulfilled.

In training school what impressed me most was the quality of my classmates which made me to realize that I am a part of a very good group. My notion of IIT graduates being intellectually superior than their peers from lesser known universities was shattered by seeing the intellectual level of some of my classmates. I saw in them exceptional clarity in their concepts and their ability of mathematical formulation of physical phenomena.

What were your aspirations when you joined DAE?

After joining the Electron Microscopy Group, I first aspired to register for the Ph.D. Programme with IIT. I think, I was the first candidate working in BARC to register for Ph.D. with IIT. In those days there were only two options before us for registering for Ph.D. Programme, one with Bombay University and the other with Banaras Hindu University (for the alumni of BHU). It was difficult for me to register for the Doctoral programme at IIT, as there was no such provision at that time. Couple of years rolled on after my applying to Kharagpur without any success. Then I wrote to Dr. Dhar requesting him to issue a Transfer Certificate, so that I can register elsewhere. On one fine day I received a letter from him that my registration process had been completed one and half years back. As a result I could save quite a bit of time for

thesis submission. Though I could not attend the courses but was allowed to take up the examinations for clearing my course requirements. Slowly over the period of time my aspirations changed. Publishing scientific papers in high impact factor journals, getting an opportunity for Post Doctoral work in reputed research institutions, making some research contributions which make a mark in the scientific literature and finally contributing towards activities related to our nuclear programme were my cherished goals.

Can you describe the life in training school in the late 60's when you joined?

Moving from Kharagpur to Trombay was a big change. At that time our stipend was 'Rs. 300/-' but we had the luxury of residing in one of the best places in Bombay – Lands End at Bandra. The accommodation was in dilapidated military barracks which were right on the sea front. During high tide, sea water used to come close to our door steps. We used to have exams on Saturdays and used to go out for a long walk or a movie on Saturday evening or Sundays. I learnt the art of preparing for the exams in one night at Kharagpur and therefore, I never felt that life in Training School was taxing.

During your career you have had the opportunity to visit many famous international labs. How would you compare the National and International Labs?

It is both hard and unfair to generalize and compare different labs. Actually the culture of an organization is not so much dependent on the country in which it is located. Each research group has its own culture. For example even within IGCAR between the two groups there will be a lot of variation. I spent one year at Max-Planck Institut fur Metallforschung, Institut fur Physik, Stuttgart, Germany during 79-80. The group I was working with, did much focused research on imaging crystal defects by Transmission Electron Microscopy. I was working on the effect of irradiation on the ordered arrangement of atoms in an alloy. I was using both heavy ions and electrons for bombarding ordered alloys and watching phase transformations induced by radiation. I met Prof. Knut Urban and started collaborative research which continued for nearly two decades. This has been the most productive scientific collaboration I had in my career. While documenting the results of my experiments, I learnt a lesson which I would never forget. Any experimental scientific paper has two distinct parts, first the observations and then the discussion. The observation within certain percentage of error is purely objective and is not dependant on the investigator. When you come to explain your observations, your imagination comes into play and the writing becomes to some extent subjective. The group I was working with never accepted a text where the observation has been mixed with discussion. Their opinion was that if you remove the discussion, your observation should still stand scientifically valid because the experiments have been done carefully and the results are reported within an error margin. Discussions come later, which is your explanation for the observed phenomenon and your interpretation can even be wrong. Making science as objective as possible was a great lesson that I had learnt from the group at MPI, Stuttgart.

They follow another practice that once a new observation is made a second person is given the task of checking the same. Such checking enhances the confidence level on the experimental observations and data. The fundamentals of scientific ethics come here in making accurate observations without any personal bias and reporting them in an objective manner. Any major discovery comes from compilations of accurate observations and their appropriate documentation. Any deviation from the expected results brings out discovery of new phenomena hitherto unknown.

You have been awarded a number of times. What is the role of awards in a researcher's life? Sir, can you recount the events leading to the Bhatnagar award.

My first award was the Young Scientist Award. It was not well known at that time as it is known today. Awards give you the excitement and further encouragement to do better. You get a kick when you receive an award. I recollect that when Dr. P. K. Iyengar asked for my Bio-data through Shri C. V. Sundaram for nominating me for the Shanti Swarup Bhatnagar Award. I was not even aware of the prestige associated with it. I was pleasantly surprised when the award came to me after a few years.

Which amongst the multitude of awards you received, you treasure the most?

Difficult to say, but considering the Indian academic scenario, I would say that Bhatnagar award is highly valuable. Recently, I received William J. Kroll Zirconium Medal from ASTM in an international meeting on zirconium alloys held in Hyderabad. This was a wonderful experience when the international community working on zirconium alloys acknowledged the contributions we made in science and technology of zirconium. I recall Prof. C.V. Sundaram telling me a few years earlier that Kroll Zirconium Medal should come to India in recognition of our work.

Your first major paper was published in Acta Metallurgica. What were your feelings? Can you recount any other event which gave you professional satisfaction?

I was obviously elated, it was my first major paper and I got the courage to send it to Acta Metallurgica only because, my mentor Dr. Krishnan asked me to do so without any hesitation. It was one of the finest moments of my life when I received an aérogram from Bruce Chalmers, the

founder editor of Acta Metallurgica with a one line statement "This is to inform the receipt of your paper and its acceptance. You will receive the proof in due course of time". I was told when the first paper from India by Asundi, Arunachalam and Krishnan was accepted in Acta Metallurgica, Dr. Brahm Prakash, the then Director of Metallurgy Group of BARC hosted a lunch for them at Taj to celebrate the occasion. My dearest colleague, Late Pradip Mukhopadhyay and I have written a book called '*Phase Transformations: Examples taken from Titanium and Zirconium Alloys*'. It took us very long to complete the work which gave me great satisfaction as it was based on our work in zirconium alloys in the last four decades.

After decades of embargo and isolation now foreign countries are opening up to India. Do, you think that slowly the world has started to realize and acknowledge the potential of Indian nuclear Industry.

Nuclear Suppliers Group was created only after the 1974 Peaceful Nuclear Experiment conducted by India. One of the main objectives was to isolate India so that the country cannot make any further progress. Thirty five years later world saw that India builds its own reactor and has the complete mastery over the entire fuel cycle. The world then realized that by introducing embargo one cannot stop Indian programme, so better to co-operate and get involved for mutual benefits. Our country is against comprehensive safeguards. On whatever technology or material we are importing our stance for safeguards is well known. The issue was regarding the placement of indigenously developed reactors and the associated fuel cycles under safeguard, which we were vehemently against. Finally, a few of our indigenous reactors along with the imported reactors are placed under IAEA safeguards and the other indigenous reactors are free from safeguards.

The international community has also realized that the embargo and isolation have not produced any desired results, so what is the use in keeping India isolated. Instead international relationships are established in nuclear commerce, participating agencies can have mutual benefits.

Also regarding safeguarded reactors, India's record has been impeccable and proliferation through India has not happened at all. Percolation of Nuclear knowhow from India to other nations has also not happened. From all these angles, India had a good case to be recognized as a responsible nuclear power.

Where do you see Indian nuclear programme 20 years from now?

We, in fact, need to grow at a faster rate. Nuclear Power Plants provide 14-15 percent of the world's electricity production. Because of embargo, our growth has been at a very slow pace and contribution of nuclear power is only 3% currently. Our base level is very low and we need to raise it to about 10% in the next two decades. This will be achieved by adding a fleet of indigenous reactors as well as setting up additional capacities through international cooperation. If we do not pick up pace now, we should not be able to build the inventory of fissile materials to embark upon a rapid multiplication through the three-stage programme. So, in the next two decades we have to make up for the time lost.

Do you think that we lack public awareness about nuclear energy in India? If yes, how do we overcome this.

Public encompasses people at multiple levels with different perceptions. Common men in street, academics, professionals, media people, politicians – for every group we have to make targeted programme. The entire programme on perception management at different levels is very extensive and good progress has been made in recent years. We have answered practically all queries from different quarters and they are all available in published reports and websites, but an impression still lingers on that our activities are covered with a veil of secrecy. We have to continue and also multiply our efforts in public awareness programmes.

Always Chairmanship was held by Luminaries. What did you feel when you took over as the Chairman?

No doubt the position of Chairman, Atomic Energy Commission and Secretary, Department of Atomic Energy was held by several luminaries starting from Dr. Bhabha. Stepping into the shoes of my illustrious predecessors had been a big challenge. I had again the good fortune to have a long association with Dr. Kakodkar from whom I learnt how to get intensively involved in a wide spectrum of activities of the Department keeping your calm. The support I received from my senior colleagues and the work culture we have in all our units in the Department were primarily responsible for smooth discharging of my duties.

What word of advice would you like to give the young engineers/scientists joining IGCAR/DAE?

My advice to you is do your work in a focussed way, without disturbing your primary focus, connect with others and set before yourself bigger goals. Working in a beautiful place like IGCAR where so many things are going on, is a wonderful opportunity for you. Strive hard and contribute for which you can be proud of, when you grow old and look back.

The team:

Ms. Vinita Daiya, Ms. Sumitra Santra, Ms. Diptimayee Samantray, Shri Anindya Bhattacharyya, Shri Ashish Shukla, Shri Avik Kumar Saha and Ms. K. Saipriya

Utilisation of Shake Table Facilities at the Structural Mechanics Laboratory

Shake Table

Shake table is used to test the response of the structures to verify their seismic performance. It will shake structural models or building components with a wide range of simulated ground motions, including reproductions of recorded earthquakes time-histories. Several kinds of shake tables are available; such as unidirectional shaker or a multi axis shake table. The modern tables typically consist of a rectangular platform that is driven in up to six degrees of freedom by servo-hydraulic or other types of actuators. A typical multi axis shake table is presented in Figure 1. The major parts of shake tables are the test bed, bearings, actuators, controllers, hydraulic power supply, reaction mass made up of concrete, computers, software, etc. The input excitations are the sine sweep, random, response spectrum and time history.

Role of the Shake Table

To make Nuclear Power Plants acceptable by the public, there is a need to meet the stringent safety criteria evolved continuously. Among the various safety aspects, the seismically induced effects call more attention at the present scenario. This has to be demonstrated by analysis and testing. Adequate full scale testing of the critical components and systems can depict a more realistic simulation. The shake tables are extensively used for the seismic qualification and research purposes. They provide the means to excite structures in such a way that they are subjected to conditions representative of true earthquake ground motions.

As far as fast reactor is concerned, the basic characteristics of particularly, sodium cooled fast reactor structures are generally thin walled shells. There are many coaxial shells, such as main vessel, thermal baffles and inner vessel with narrow annular space confining liquid sodium. The large size vessel supported at one end, carrying a large sodium mass and presence of narrow

annular gaps filled with sodium, generate maximum dynamic amplification during a seismic event. To capture the seismic response of the structures more realistically, particularly, the dynamic behaviour due to the presence of narrow annular gaps filled with sodium, large scale testing is required. Towards that, large size test bed will help in conducting the integrated testing of the reactor assembly with more internals like Control and Shutdown Rod Drive Mechanism (CSRDM) etc. Thus, a large size and large capacity shake table is preferred for raising the confidence and structural Integrity of the fast reactor components under seismic excitations.

Status of the Structural Dynamic Test Facilities at SML

Structural Mechanics Laboratory (SML) is extensively involved in the structural dynamic studies also. Many seismic qualification and research tests have been carried out with comparatively less time involved. These tests were conducted at the SML, using the 2 T capacity unidirectional electro dynamic shaker and 10 T capacity tri-axial servo hydraulic shake table. The photograph of the 2 T capacity uni-axial shaker along with the sub-assembly (SA) experimental models is given in Figure 2a and the 10 T multi axial shake table along with the 1/8th scale down model of the Prototype Fast Breeder Reactor (PFBR) Main Vessel (MV) is shown in Figure 2b.

The installation and commissioning activities of the high capacity shake table is under progress at SML. The main feature of this shake table bed is having a centre hole. So that the top supported cylindrical hanging components can be directly mounted on the shake table and the specimen centre of gravity from the table top can be reduced. Providing additional rigid support to simulate the support condition can also avoid with this arrangement.

High capacity shake table is basically a servo-controlled hydraulically actuated shake table having the table size of

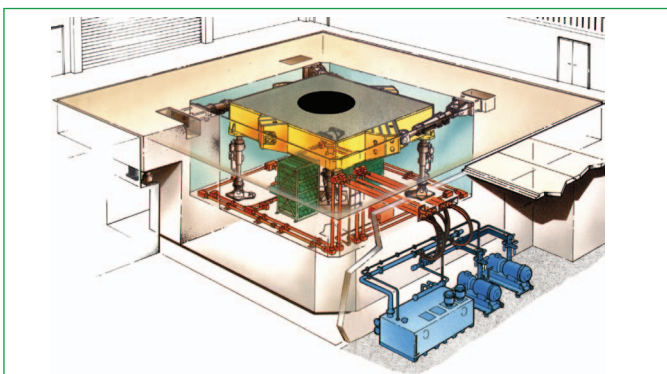


Figure 1: A typical multi axial shake table

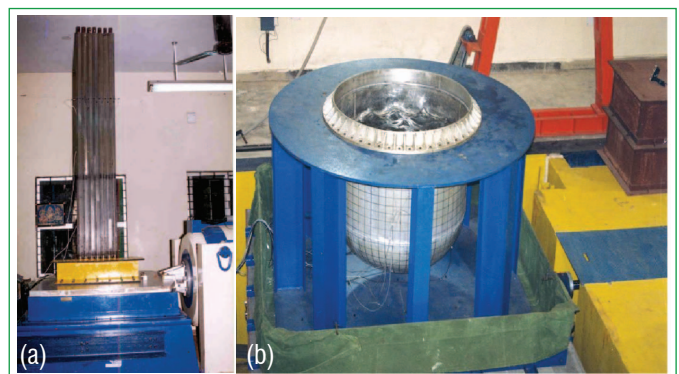


Figure 2:(a) Unidirectional electro dynamic shaker with sub-assembly models and (b) multi axis shake table with 1/8th model of main vessel

Table 1: The major technical specifications of the structural dynamic test facilities

Items	Uni-axis Shaker	Multi axis Shake Table		Multi axis High Capacity Shake Table	
Status	Under Operation	Under Operation		Under Installation	
Mode of actuation	Electro dynamic	Servo Hydraulic		Servo Hydraulic	
Pay Load – ton	2	10		100	
Table Size – metre	1 x 1	3 X 3		6 X 6	
Height of specimen centre of gravity from table top – metre	0.5	2		2	
Frequency – Hz	1000	60		60	
Shaking direction	Single	2 Horizontal	Vertical	2 Horizontal	Vertical
Displacement – millimetre	± 25	±150	±100	±150	±100
Velocity – m/s	-	±0.3	±0.3	±1.2	±0.9
Acceleration – g	± 3.0	±1.5	±1.0	±1.5	±1.0

6 X 6 m with a maximum payload testing capacity of 100 T. The major technical specifications of the structural dynamic test facilities available at SML, are presented in Table-1.

Utilisation of the Shake Table Facility at SML

The shake table facilities available in SML have been extensively used for various seismic qualification and research type experimental purpose. The qualification experiment mainly covers the experiments carried out for the components fabricated by various industries mainly M/s. MTAR, M/s. ECIL, M/s. BEL, M/s. MAGTORQ, M/s. BS&B etc. towards BHAVINI, Kalpakkam for the Fast Breeder Reactor (FBR) programmes and for NPCIL, Mumbai for the PHWR programmes in India. Apart from the qualification tests, the table has been extensively utilised for the research and development activities of IGCAR and other national institutes in India. Even with comparatively less man power involvement, during the last four years more than forty experiments have been completed using this 10 T shake table.

Qualification Tests

The seismic qualification tests carried out as per the test procedure given in IEEE STD 344-1987 standards. IEEE recommended practice for seismic qualification of class 1E equipment for

Nuclear Power Generating Station. It includes the resonance search test followed by five operating basis earthquake (OBE) and one safe shutdown earthquake (SSE) for the components designed for seismic category-1. The SSE test is not required for the components designed for seismic category-2. A respective spectrum compatible time history will be generated for both OBE & SSE in all the three orthogonal directions. Towards that enveloped and broadened floor response spectra (FRS) available on the support condition of the component at the specified damping will be used. The input time history for the base excitation is generated such that the test response spectra (TRS) shall envelope 10% more than the required response spectra (RRS) in all the frequency range given in the envelope FRS as per the standard procedure requirements. Both functional and structural integrity will be ensured towards seismic qualification. Strain gauge pasted at the critical locations helps in ensuring structural integrity. The component response under testing will be captured using the tri-axial accelerometers provided at the selected locations.

Some of the important recent seismic qualification experiments conducted towards the FBR program are listed below:

- Various types of valves (Figure 3) have been tested using this

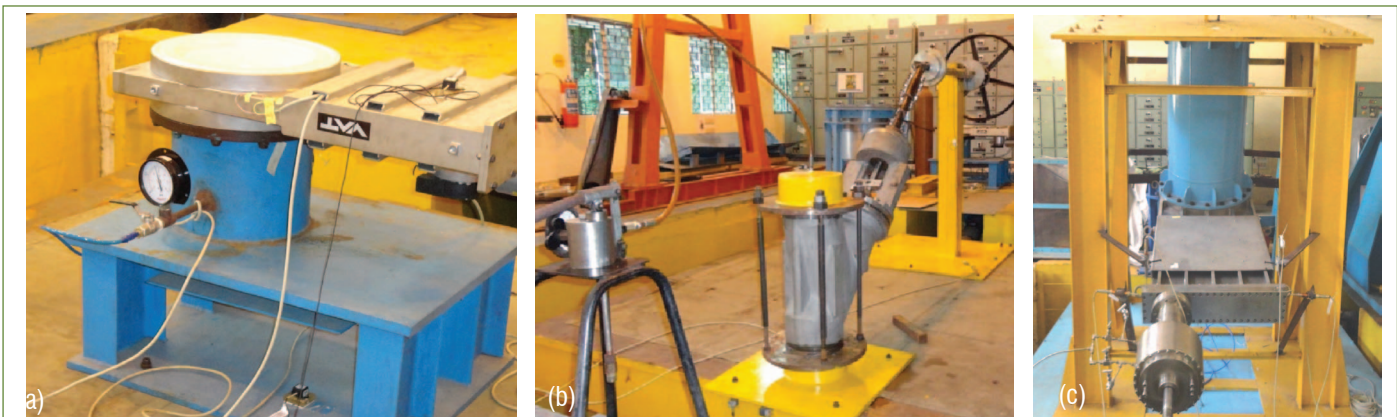


Figure 3: Various valves tested for PFBR (a) VAT table, (b) extended steam valve and (c) IFTM table

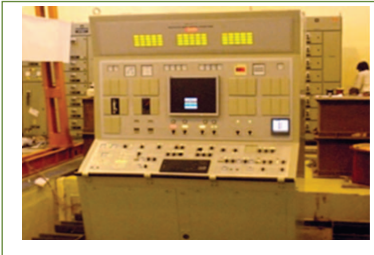


Figure 4: PFBR main control panel



Figure 5: (a) Rotatable plug gear boxes (b) safety vessel insulation panel and (c) PFBR electrical penetration assembly

table to meet PFBR seismic design requirements which include mainly the VAT valves, which are provided in the fuel transfer cell (FTC) of the PFBR for isolation purpose, extended steam valves, provided inside cells of the PFBR reactor containment building (RCB) for sodium pipings and inclined fuel transfer machine (IFTM) gate valve, provided in the IFTM to maintain the pressure boundary integrity of the RCB

- The other important components tested for the PFBR qualification are the main control panel (Figure 4), permanent magnetic flow meter along with the associated pipe segment, public address system, underwater trolley motor drive assembly used to transfer spent sub assembly to the storage bay, remote terminal unit and junction boxes deployed to acquire the process data, 400 terminal and 150 terminal junction boxes for power supply inside RCB, PFBR lighting components etc.
- Many indigenously developed components for the PFBR also have been qualified using this shake table. PFBR rotatable plug gear box drive assembly (Figure 5a), safety vessel thermal insulation panel (Figure 5b) and electrical penetration assembly (Figure 5c) are a few among them. PFBR large rotatable plug and small rotatable plug drive mechanisms provided with suitable gearboxes with drive motors to locate the transfer arm over any desired core subassembly location. This mechanism (Figure 5a) has been qualified for five OBE excitations towards ensuring the functionality requirement under seismic condition. Stainless steel plate type thermal insulation panels that are mounted on safety vessel, to limit the heat flux to reactor vault concrete, has been qualified under seismic excitations caused due to OBE as well as SSE. The single panel without considering the constraints offered by the adjacent panels

is presented in Figure 5b. The photograph of the electrical penetration assembly is given in Figure 5c

- Various field instruments for pressure, flow, temperature and level measurement also qualified against the seismic conditions as per the technical specification of sodium and miscellaneous piping package instrumentation
- The important seismic experiments conducted for the Fast Breeder Test Reactor (FBTR) are the qualification of RCB damper and the Butterfly valve
- Seismic qualification of the control panel and the Exide battery bank are the experiments conducted towards the DFRP systems and components
- Seismic qualification of the rupture discs for the KAPP-3&4 & RAPP-7&8, spent fuel storage trays of PHWR and Prototype electronic cabinet for the KAPP-3&4 are the recent experiments conducted towards the PHWR applications (Figure 6). The various category rupture discs were tested, which included the rupture disc size of 15 NB, 1", 2" and 4". It is mainly used for the primary piping package of the KAPP-3&4 & RAPP-7&8. 20" tested rupture disc is used to safeguard the Calandria pressure vessel under the postulated extreme condition of pressure surge.

Research & Development Activities

The shake table has been extensively used for the in-house R&D activities also. Some of the important experiments conducted in this category are given below:

- One of the noted phenomena demonstrated experimentally in this category is the free level sloshing due to dynamic instability (Figure 7). For some combinations of the frequency

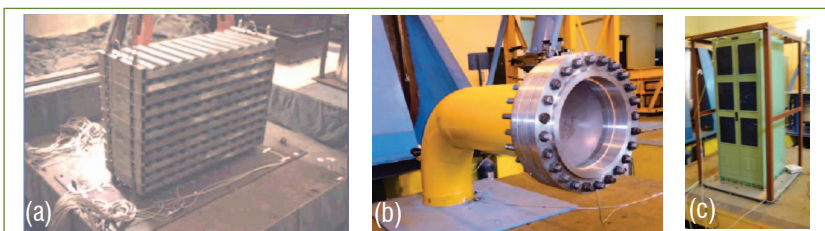


Figure 6: Typical seismic qualification for the PHWR components (a) spent fuel storage trays (b) OPRD for Calandria and (c) prototype electronic cabinet

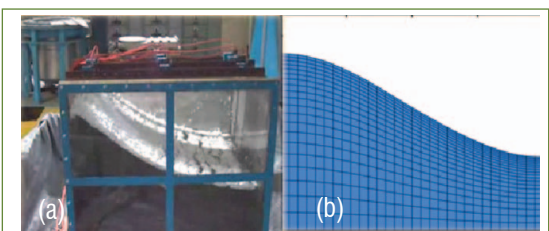


Figure 7: Rectangular tank under vertical excitation by (a) experiment and (b) 2D numerical model

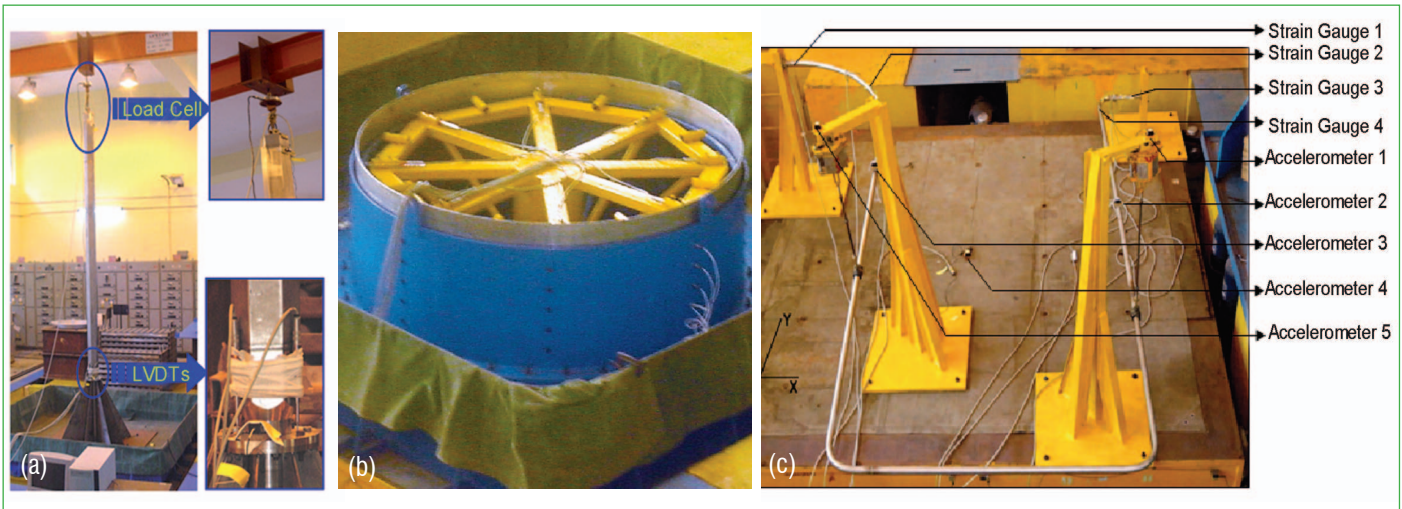


Figure 8: Various components of PFBR tested in the Shake Table (a) PFBR sub-assembly, (b) dynamic pressure distribution in thermal baffle and (c) typical FBR multi supported pipe line

and amplitude, the response of the free surface is unbounded leading to instability called dynamic instability or parametric instability, and for other combinations the response is bounded i.e. stable.

- The study of possibility of the upward displacement of PFBR sub-assemblies relative to grid plate under the combined effect of upward fluid force and vertical seismic excitations due to SSE. The experimental setup is given in Figure 8a
- Shake table experiments were conducted to study the development of dynamic pressure along the circumference of the narrow annular gap geometry filled with water under seismic loading (Figure 8b). The study simulates the narrow annular space available with the thermal baffle filled with sodium
- The experimental layout of the shake table towards the

benchmark studies carried on a typical FBR piping layout under multi supported condition is shown in Figure 8c

- The IGCAR shake table has been extended for other DAE units applications also. One of the experiments in this category is the ITER (International Thermonuclear Experimental Reactor) blocks tested to check the loosening of the bolts under dynamic loading and it is presented in Figure 9.

The shake table facility available at SML has been used for various seismic qualification tests. This covers mainly the tests carried out for the conventional components and equipment and also for the many indigenously developed experiments and equipment for the FBR, PHWR programmes and other national interests in India. Apart from the qualification experiments, the shake table has been extensively utilised for the Research and Development activities of IGCAR and other national institutes in India. During the last four years more than 40 experiments have been completed using this 10 T shake table relatively within a shorter duration, so that it helps in accelerating the PFBR schedule.

To capture more realistically, the dynamic behaviour due to the presence of narrow annular gaps filled with fluid, fluid-structure interaction, free level sloshing etc, large scale testing is required. Thus the 100 T capacity high capacity multi axis shake table will help in conducting the integrated testing of the reactor assembly more realistically. By integrating both the 10 T and 100 T shake table together will help in performing more realistic multi support excitation experiments also. This helps not only in raising the confidence of the public towards the acceptance of future nuclear power plants but also ensures the structural integrity of the fast reactor components under severe seismic conditions.

*Reported by P. Chellapandi and colleagues
Reactor Design Group*



Figure 9: Testing of ITER blocks

Impression Creep: An Innovative Testing Technique for Evaluation of Creep Properties of Materials

Uniaxial creep testing technique is the most commonly used test method for characterization of creep deformation behavior of materials. The test specimens used for these studies are of standard geometry, require a considerable volume of material for specimen preparation and the tests are carried out generally as per ASTM standard E 139 procedures. Further, it requires many such specimens to carry out creep tests at different temperatures and stress levels in order to assess various creep deformation parameters. Hence, the test methodology is both time and material consuming. As a result, where the amount of material available for testing is small or in the case of rapid screening of several laboratory heats for development of new alloys, small sized specimen testing techniques are attractive. Impression creep testing technique is an innovative miniature testing technique that can be used to study the creep deformation behavior of materials. This method cannot be used for determining creep rupture life and rupture ductility.

Impression Creep Test Technique

In an impression creep test, a constant load (L) is applied to the test specimen through a flat-ended cylindrical indenter at high temperature. The depth of penetration (h) of the cylindrical punch is recorded continuously as a function of the elapsed test time. A plot of depth of penetration versus time, gives the impression creep curve. The impression creep curves are similar to the conventional creep curves, but they exhibit only the first two characteristic stages of the conventional creep curve, namely, the primary and secondary creep stages. There is no tertiary creep stage in an impression creep curve. This is because of the fact that in an impression creep test, loading is compressive in nature. As a consequence, creep cracks and necking of specimen which occur during the tertiary creep stage leading to fracture do not take place. The rate at which the cylindrical punch penetrates into the test specimen is controlled by the time dependence of the movement of the material under the punch and thus directly monitors the creep behavior of the localized volume of the material beneath the indenter.

Advantages and Limitations of Impression Creep Technique

Impression creep technique has several advantages when compared with conventional creep tests such as

- i) It is material non-invasive and hence requires a small specimen for the tests; hence it is attractive for remnant life assessment studies where it is not desirable to remove large amount of material from an operating component
- ii) It enables rapid screening of creep properties of small laboratory heats for optimizing the chemical composition in

any alloy development programme since impression creep test time is relatively short

- iii) Characterization of creep properties of different and narrow microstructural regions in the heat affected zone of weld joints, which is not possible to be determined in conventional creep tests
- iv) A large amount of creep data can be collected from one sample which not only reduces the effort for sample preparation, but also reduces the sample to sample scatter in properties
- v) Because of the small indentation left in the specimen, the technique is in a sense nearly non-destructive; the small amount of compressive residual stresses remaining after the tests is not considered to be deleterious.

Despite these advantages, impression creep technique has limitations such as

- i) Type of loading is compressive unlike in conventional creep tests where the loading is tensile
- ii) Rupture life cannot be determined by this technique because there is no fracture of the sample
- iii) Since the test time is generally short, typically about a few hundreds of hours, creep behaviour due to long time concurrent microstructural changes occurring in engineering alloys at high temperatures cannot be captured
- iv) Although the test is relatively easy to perform and requires shorter time, interpretation of the results is difficult on account of the complex multi-axial nature of the stress beneath the indenter and the continuously varying amount of material under the indenter which is experiencing elastic, plastic and creep deformation.

Impression Creep Testing Facility

A unique impression creep testing facility has been developed and it consists of two identical machines. The impression creep machine consists of a vacuum system (up to 10^{-6} mbar) which is used to avoid oxidation of the specimen at higher test temperatures. The furnace is located inside the vacuum chamber. Inside the furnace, there is a specimen cage which consists of two rigid frames, one fixed to the bottom plate of the specimen cage and the other connected to the pull rod which is free to move. The former has an indenter holder to which the indenter is fixed and the latter has a sample holder over which the test specimen is placed exactly below the indenter. The flat-ended cylindrical indenters are made of tungsten carbide and have typically 1 mm diameter. The pull rod is connected to the lever arm which has 1:10 lever ratio. The vertical movement of the pull rod and hence

the impression depth is monitored through a linear variable differential transducer with an accuracy better than $\pm 0.5\%$. The maximum capacity of the load cell which is attached to the load train is 1 kN. The temperature controller is capable of maintaining the temperature on the specimen constant with an accuracy of $\pm 1^\circ\text{C}$. Data is collected and recorded using a PC-based online data acquisition system (The equipment is shown in Figure 1).

Analysis of Impression Creep Parameters

In an impression creep test, a constant load L is applied to the test specimen through a cylindrical punch of diameter d . The mean pressure under the punch is referred to as the punching stress and is given in equation 1 of Table 1. Due to the punching stress, σ_{imp} the cylindrical punch penetrates into the surface of the test specimen to a depth h in time t . The rate at which the cylindrical punch penetrates the specimen surface is referred to as impression velocity and is given as equation 2.

For the characterization of creep behavior of materials using impression creep test, it is essential to establish correlations between the impression creep parameters (σ_{imp}, v_{imp}) and uniaxial creep stress (σ_{uni}) and uniaxial steady state creep rate ($\dot{\epsilon}_{uni}$). The general forms of these correlations are given as equations 3 and 4, where, α and β are the correlation factors. For most engineering materials, values of α range from 0.26 to 0.36 and $\beta = 1$. In the present analysis, we used the conversion factors $\alpha = 0.33$ and $\beta = 1$, to correlate the creep data from impression and conventional uniaxial creep tests. The plot of steady state impression velocity versus punching stress on a log-log scale gives a straight line with a slope equivalent to the stress exponent, n_{imp} shown as equation 5.

Impression Creep Studies on 316LN SS

Impression creep tests have been carried out at 650°C on four heats of 316LN SS containing 0.07, 0.11, 0.14 and 0.22 wt.% nitrogen, under different punching stress levels ranging from 400-800 MPa, using specimens of nominal dimension $20 \times 20 \times 10$ mm. Impression creep tests have also been carried out on the heat-affected zone, the weld metal and the base metal of a 316LN SS weld joint at 650°C . All the experiments were carried



Figure 1: Impression creep testing machine developed at IGCAR

out in vacuum (10^{-6} mbar) in order to avoid the oxidation of the specimen.

Correlation between Impression Creep Results and Uniaxial Creep Results

Typical impression creep curves, presented as variation of punch penetration depth with dwell time, under different punching stress levels, are shown in Figure 2a. The longest test time in the investigation was about 1000 hours. The slope of steady state portion of impression creep curve, which is referred to as steady state impression velocity, was calculated for each stress level. Figure 2b shows the plot of steady state impression velocity versus punching stress on a log-log scale. A power law relationship was found to be obeyed with a power law exponent value of 6.4. The punching stress and the steady state impression velocity have been converted to equivalent uniaxial stress and uniaxial steady state creep rate using equations (3) and (4), respectively. Figure 2c shows excellent correlation between uniaxial steady state creep rate and equivalent steady state creep rate obtained from impression creep tests for 316LN SS containing 0.14 wt. % nitrogen. Although rupture life cannot be determined from impression creep tests, the well-known Monkman-Grant relationship between steady state creep rate and rupture life exhibited by most materials can be used to estimate the rupture life using steady state creep rates determined from impression creep tests. Figure 2d shows the relation between steady state creep rate and rupture life for 316LN SS containing 0.14 wt. % nitrogen based on uniaxial creep tests.

Influence of Nitrogen Content on Creep Behavior of 316LN SS

Figure 3a shows the variation of equivalent steady state strain rate with equivalent stress (derived from steady state impression velocities and punching stresses using equations (3) and (4)). A dislocation creep mechanism was found to be obeyed (as identified by the value of n) which was also observed earlier from

Table 1: Equations

$\sigma_{imp} = \frac{4L}{\pi d^2} \quad (1)$	$\dot{\epsilon}_{uni} = \frac{v_{imp}}{\beta d} \quad (4)$
$v_{imp} = \frac{dh}{dt} \quad (2)$	$n_{imp} = \left(\frac{\partial \ln(dh/dt)}{\partial \ln \sigma_{imp}} \right) \quad (5)$
$\sigma_{uni} = \alpha \sigma_{imp} \quad (3)$	

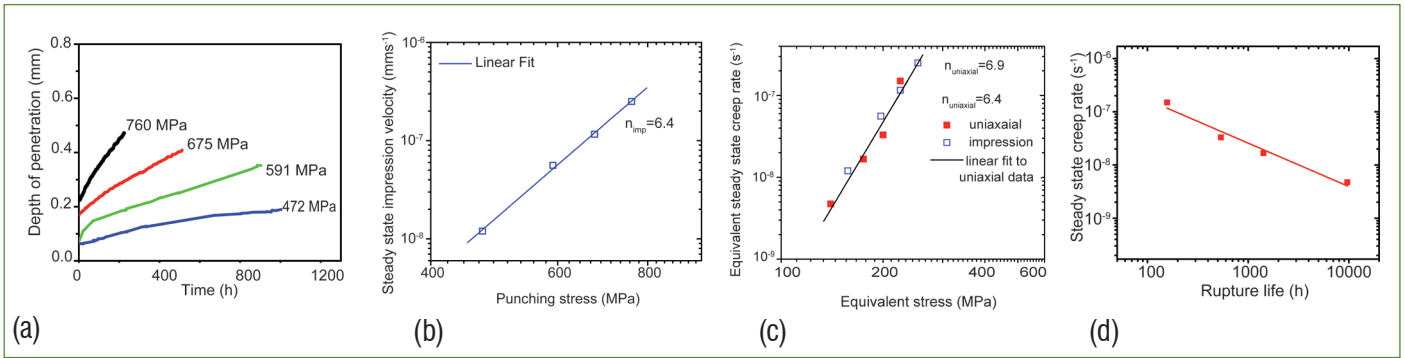


Figure 2: (a) Typical impression creep curves for 316LN SS at 650° C containing 0.14 wt. % nitrogen at various stress levels, (b) plot of steady state impression velocity versus punching stress, (c) correlation between uniaxial steady state creep rate and equivalent steady state creep rate obtained from impression creep tests and (d) variation of steady state creep rate with rupture life from uniaxial creep tests

uniaxial creep tests. Figure 3b shows the variation of equivalent steady state creep rate with nitrogen content at different stress levels. It was observed that the equivalent steady state creep rate decreased with increasing nitrogen content at all the stress levels. These results are found to be in good agreement with the results obtained from conventional uniaxial creep tests. Impression creep testing technique was thus found to be sensitive to capture the variation in creep rate due to very small change in the nitrogen content in 316LN SS in the alloy development programme.

Creep Behavior of 316LN SS Weld Joint

Impression creep tests have been carried out to characterize creep deformation behavior of different microstructural zones of 316LN SS weld joint. The microstructure of the weld joint was characterized by equi-axed grains in the base metal; the heat-affected zone consisting of coarse grains and the weld metal consisting of duplex microstructure of delta-ferrite in austenite matrix observed using optical microscope. Impression creep tests have been carried out at 650°C on the weld metal, the base metal and the heat-affected zone. The weld metal, the base metal and the heat-affected zone exhibited distinct creep behaviors (Figure 4a).

Figure 4b shows the variation of impression velocity with time for the three microstructural zones. It is clearly evident that the weld metal deforms at the highest creep rate and the heat-affected zone at the lowest rate, thereby demonstrates that impression creep is a reliable technique to evaluate the creep behavior of different narrow microstructural zones.

It can be concluded that the weld metal will have the lowest rupture life and the base metal will have the higher rupture life; these conclusions are in agreement with results from uniaxial creep tests carried out on base metal and weld metal separately.

A unique impression creep testing facility has been developed and has been employed to characterize the creep behavior of type 316LN SS and different microstructural regions of the weld joint. A good correlation has been established between the impression creep and uniaxial creep data. Impression creep technique was proved to be an efficient material non-invasive technique to characterize creep deformation behavior.

*Reported by M. D. Mathew and Colleagues
Mechanical Metallurgy Division
Materials Development and Technology Group, MMG*

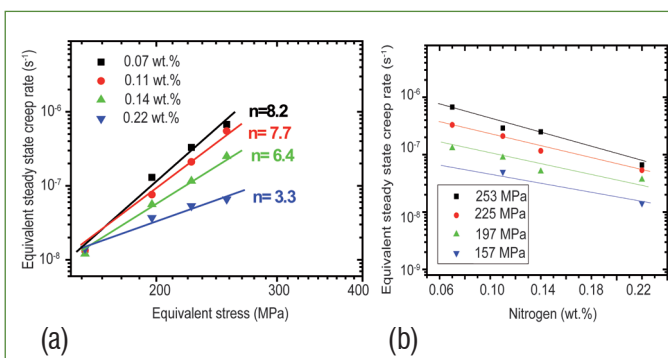


Figure 3: (a) Plot of equivalent steady state creep rates and uniaxial tensile stresses derived from steady state impression velocities and punching stresses and (b) variation of equivalent steady state creep rates with nitrogen content in 316LN SS for various stress levels

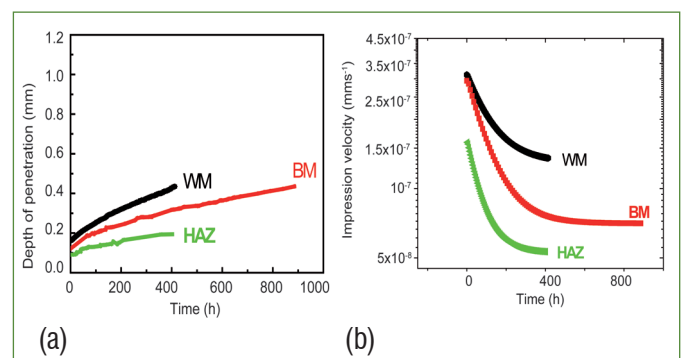


Figure 4: (a) Typical impression creep curves for the weld metal, the base metal and the heat-affected zone and (b) impression velocity vs time curves in 316LN SS weld joint

Young Officer's FORUM

Investigation of Structural and Optical Properties of ECR-CVD Grown Ultra Smooth Diamond-like Carbon Films

In recent past the carbon based nanostructures and thin films have gained a lot of interest. Atomic carbon can exist in three relatively well-known allotropes such as amorphous carbon, graphite and diamond. Some of the widely researched carbon structures are fullerenes, buckyballs, carbon nanotubes, carbon nanobuds and nanofibers. Several other exotic allotropes such as lonsdaleite, glassy carbon, carbon nanofoam and linear acetylenic carbon (carbyne) have also been discovered. The physical properties of carbon vary widely with the allotropic form. For example, diamond is highly transparent, while graphite is opaque and black.

Diamond-like carbon is a name attributed to a variety of amorphous carbon materials with broad range of properties. This can range from graphite-like to diamond-like (tetrahedral amorphous carbon) to polymer-like. The "diamond-like carbon" term is commonly used to designate the hydrogenated form of diamond-like carbon (a-C:H), while the "taC" (tetrahedral carbon) term is used to designate the non-hydrogenated with high fractions of sp^3 hybridized carbon thus they possess properties close to diamond. In the recent times, interest in diamond-like carbon films has grown significantly because of their superior properties used in applications of technological importance. For instance, their high chemical inertness, superior mechanical properties, low friction coefficient, high optical transparency, tunable electronic properties, make them potential candidate for protective coatings on magnetic storage disks, as low friction and wear resistance coatings for tribological tools, as antireflective coatings for solar cells, electroluminescence materials, field emission devices, biosensors and biomedical coatings. The physical properties of diamond-like carbon films can be tuned by controlling the sp^3/sp^2 ratio. The properties of diamond-like carbon films are highly sensitive to process conditions. Though it appears to be a problem, on the other hand it offers the opportunity to tailor the coating properties to specific applications. Various deposition techniques like magnetron sputtering (DC or RF), pulsed laser deposition, ion beam deposition, filtered cathodic arc deposition, hot filament chemical vapor deposition (CVD), microwave enhanced plasma CVD and electron cyclotron resonance plasma



Shri Syamala Rao Polaki, obtained his M. Tech in Materials Science from IIT Bombay, in 2007. He joined IGCAR as DAE Graduate Fellow in 2007 and is currently working as Scientific Officer in SND/MSG. His current area of interest is synthesis of nano-crystalline diamond and diamond like carbon thin films for tribology applications.

CVD (ECR-CVD) are employed for the synthesis of diamond-like carbon thin films. Among all the methods, ECR-CVD is the most preferred technique because of its high plasma density, larger deposition area, superior electron temperatures and flexibility in operating at lower pressures. Moreover, as ECR-CVD doesn't consist of any electrodes, it enables us to maintain the substrate at a desired voltage, which in turn helps to tune the ion flux density and energy independently.

An attempt has been made to grow diamond-like carbon films on Si(100) substrate using electron cyclotron chemical vapor deposition. The aim was to grow ultra smooth diamond-like carbon films with high sp^3 content even at very low film thicknesses. As the growth conditions potentially control film properties, we tried to achieve our aim by growing the diamond-like carbon films at different ion energies and reactive gas concentrations. The typical deposition conditions are base pressure 1×10^{-6} mbar, CH_4 : Ar mixture 5:10, 10:10 and 20:10 sccm (standard cubic cm per minute) and microwave power 300 and 400 W. These samples will subsequently be denoted as S300-5, S300-10, S300-20, S400-5, S400-10 and S400-20 where the first term represents the microwave power (Watt) and the second term represents the methane flow in sccm. All the films were grown at deposition pressures of about 3×10^{-3} mbar and a -100 V substrate biasing for a duration of one hour.

The grown diamond-like carbon films were characterized by AFM, FESEM, Raman spectroscopy and RBS to study their topography, surface roughness, morphology, thickness and properties. The Figure 1 illustrates a typical AFM topographic image of the film S300-10. The topography studies confirm that all the films are uniform and smooth without any crystalline features. The surface roughness analysis shows that the films are ultra smooth with the root mean square (rms) roughness in the range of 2.2 to 2.5 Å. Low rms values are attributed to the salient features of ECR-CVD namely the controlled growth process and low deposition rates < 1 nm per minute. ECR-CVD is also known for the constant ion energy with narrow ion energy distribution

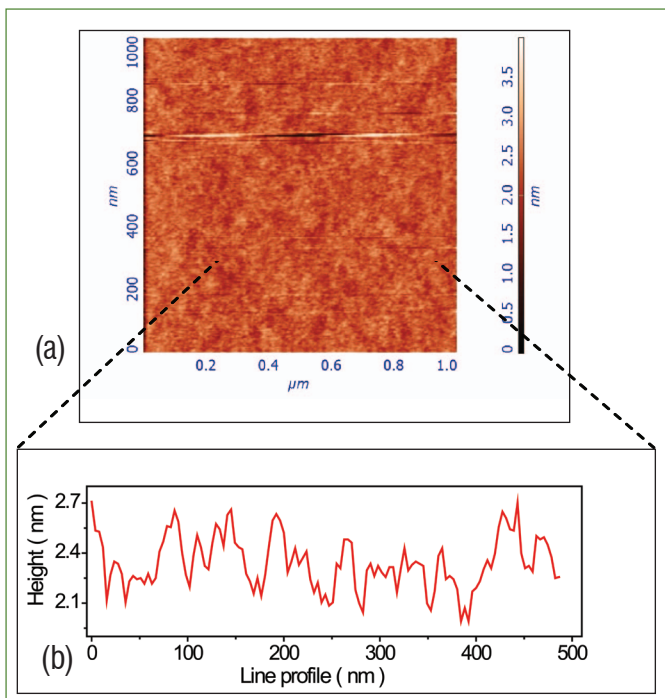


Figure 1: (a) AFM topography of the DLC film exhibiting ultra smooth surface with rms roughness 2.4 \AA (b) height profile across the line indicated in the topographic image

(few eV), especially when the substrate is biased with a DC voltage and which is the dominant factor to result in the ultra smooth films. Because the dissipation of energy by high energy ions is by transmitting the heat and generating thermal spikes ($\sim 1 \text{ ps}$) in atomic length scale cause local melting that results in the ultra smoothness in the films. The slower growth rates ($< 1 \text{ nm per min}$) could provide sufficient time for dissipation of the ion energy uniformly throughout the film. Moreover the atomic displacement energies for graphite and diamond are 25 and 80 eV, respectively, which are less than the ion energy in our experiments.

The surface morphology and thickness of these films are directly measured by FESEM. The Figure 2a shows the typical surface morphology and cross sectional image (shown in the inset) of the film S300-10. SEM image confirms that the films are uniform, smooth and free of pinholes over a large area. From the cross sectional FESEM images, the thickness of the films are found to be in the range of 13 to 62 nm, depending on the growth conditions. The observed variation in film thickness with change in methane concentration and microwave energy is shown in Figure 2b. In general, in the growth process of the diamond-like carbon films by plasma based techniques, the chemical etching and deposition compete with each other and the dominant mechanism determines the growth rate, morphology and the quality of the films. In the case of the films deposited at 300 W microwave power, the increase in methane flow rate from 5 to 10 sccm resulted in increase of thickness from 40 to 62 nm.

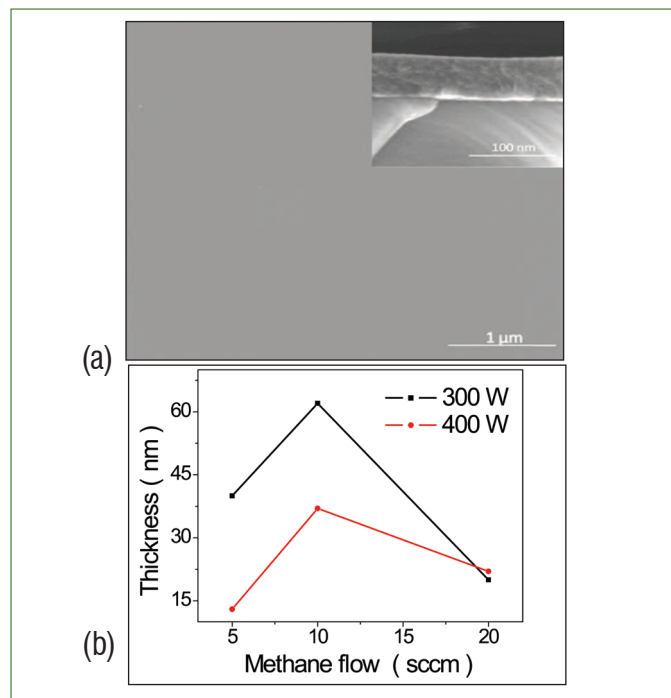


Figure 2: FESEM (a) morphology and (b) thickness variation with respect to methane flow rate with inset in showing the cross sectional micrographs of S300-10

This is attributed to the increase in the concentration of carbon radicals in the plasma. When the methane flow is further increased to 20 sccm, there is a rapid decrease in the film thickness (to 20 nm) which can be attributed to the drastic increase of the hydrogen ion concentration in the plasma due to the dissociation of higher amount of methane. The hydrogen ions are known for their etching nature of the graphitic carbon and also it can even decrease the CH_3 radical ion concentration by chemically reducing it back to CH_4 , known as passivation of dangling bonds. A similar trend in thickness variation is also observed for the films deposited at 400 W microwave energy. However, the film S400-5 shows the lowest thickness of 13 nm which could be attributed to the resputtering of the films by higher Ar^+ ion flux / energy as well as the lesser concentration of the carbon radicals in the plasma due to lower content of methane in the reaction mixture. In addition to the physical sputtering by energetic ions, chemical etching of the films due to hydrogen ions also responsible for the growth rate as well as film quality.

Detailed structural properties of the films are studied by Raman spectroscopy. The Figure 3 depicts the typical Raman spectrum of the film S300-10. The observed Raman spectrum is deconvoluted into two peaks at around ~ 1350 and 1530 cm^{-1} using Gaussian fit. The peaks at 1350 and 1530 cm^{-1} are corresponding to characteristic D and G bands of amorphous carbon films. A similar deconvolution is performed for all the samples and their G-peak position, FWHM of G peak and I_D/I_G ratio were obtained and analyzed. All the films exhibited the

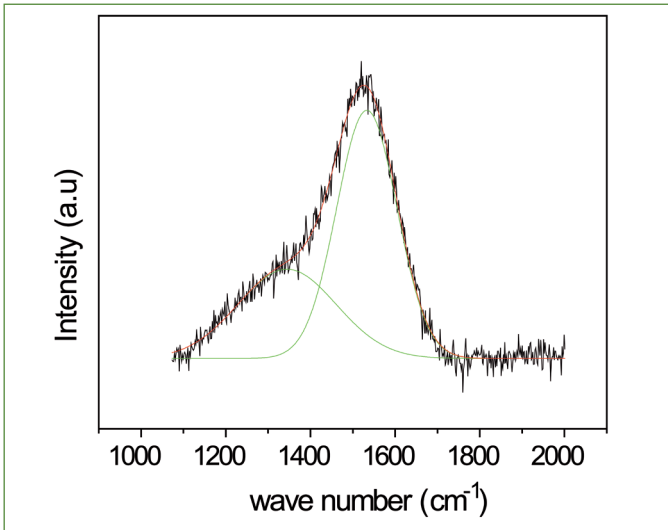


Figure 3: Raman spectrum of the DLC film of S300-10

G peak position at lower wave number (around 1530 cm^{-1}) than that of sp^2 bonded graphitic structure (1580 cm^{-1}) which indicates that the samples consist of higher sp^3 fraction. It is observed that the increase in microwave energy introduces blue shift in G peak (higher wave number) increases the I_D/I_G ratio, which indicates the reduction in defect density, increase in sp^2 bonded crystallinity and converts to more graphitic in nature. The higher microwave energy increases ion density as well as ion bombardment on to the film surface which might make the films denser. Nevertheless, the internal stress that exists in the films also plays an important role in deciding the position of G peak. Here, we analyze the quantitative information obtained by Raman studies on diamond-like carbon films with respect to thickness only.

Figures 4a to 4d shows the thickness dependant of G peak position, I_D/I_G ratio, FWHM and peak intensity, respectively. Figure 4a shows the increase of G peak position with decrease in the film thickness which can be attributed to the stress present

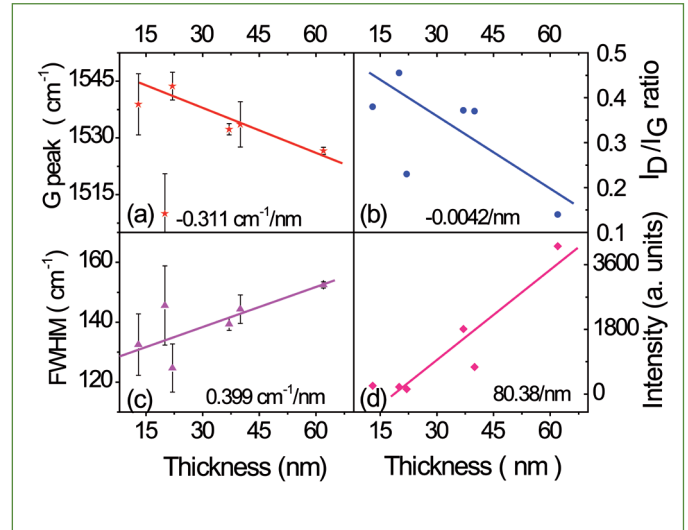


Figure 4: Thickness dependent (a) G peak position (b) I_D/I_G ratio (c) G peak FWHM and (d) I_G peak intensity for the grown DLC films derived from Raman spectroscopy

in the films. When the thickness decreases, the interfacial tension introduces large compressive stress on the films and it gets relaxed when the thickness increases. It should be noted that the shift in G peak position either could be due to stress or bonding in the diamond-like carbon films. Hence, it is very difficult to exactly identify the factor which caused the shift in G peak position by Raman spectra alone. The I_D/I_G ratio decreases with increase in thickness as shown in Figure 4b this is attributed to increased sp^3 bonding. Also, the G peak intensity and its FWHM increases with thickness as shown in Figures 4c and 4d, respectively. It indicates that the disorder increases with thickness due to the increase in sp^3 bonding and also it confirms the reduction of sp^2 crystallites in the films. Overall, these observations suggest that the quality of these diamond-like carbon films is improved with the increase in film thickness.

Rutherford Back scattering (RBS) spectroscopy studies are carried out to obtain the thickness of the films (normalized

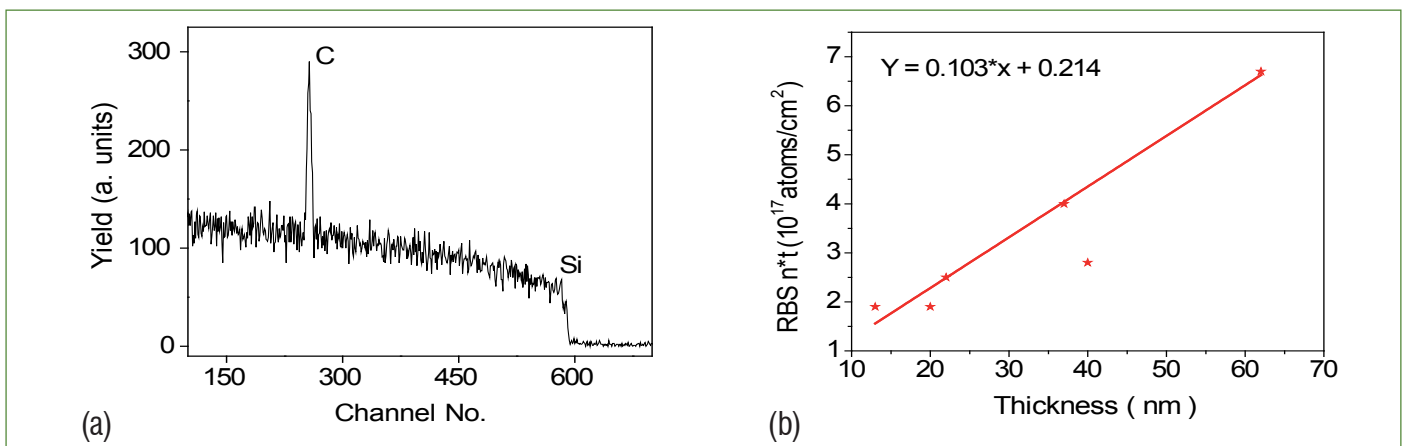


Figure 5: (a) Typical RBS spectrum of a DLC film and (b) RBS thickness versus physical thickness of the DLC films

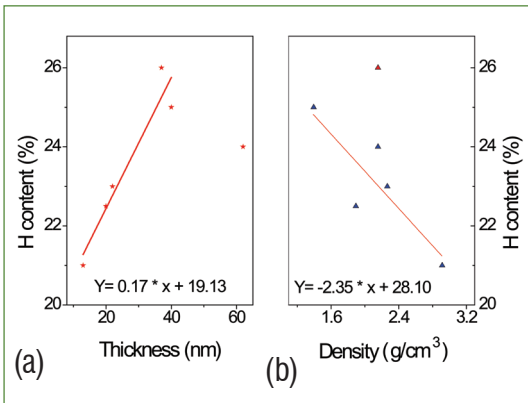


Figure 6: The variation of hydrogen content with respect to (a) physical thickness and (b) density of the films

to number density per unit volume and multiplied by the films thickness – $n \cdot t$, atoms/cm²). Figure 5a shows a typical elemental depth profile by RBS spectrum of the sample S300-10. The RBS thicknesses of the films are found to be in the range of $1.9 - 6.7 \times 10^{17}$ atoms/cm². The peak around channel number 250 denotes the carbon and the shoulder around channel number 600 corresponds to Si. The RBS film thickness shows a linear relation with the physical thickness and that is shown in Figure 5b. Density of these films is obtained by dividing the RBS thickness with absolute film thickness (measured by FESEM). The film S400-5 has shown the highest density and this is attributed to the higher Ar⁺ ion bombardment. However, the density of the films deposited at higher ion density is higher for all the methane flow rates this is due to the increase in higher ion bombarding rate.

It is very difficult to avoid hydrogen in the diamond-like carbon films and the extent of its concentration greatly influences the properties of the films. So the quantitative estimation of hydrogen is vital to assess the quality of the diamond-like carbon films. In the present study, elastic recoil detection analysis (ERDA) is used to estimate the hydrogen content in the films grown on Si substrates and the measured its concentration is in the range 21 to 26%.

An increase in hydrogen content is observed with film thickness as shown in Figure 6a. The variation hydrogen content is also linear with the density of the films estimated from the RBS studies and shown in Figure 6b. These results indicate that the hydrogen content in the films helps to stabilize the sp³ bonding and thereby influences their density. These observations are in support with the Raman analysis. Figure 7a shows typical UV-Vis-NIR transmittance spectra of the diamond-like carbon films deposited on to quartz substrates. It is evident that all the films exhibited high transmittance ($T > 97\%$) in the wavelength range 500 to 900 nm. The optical band gap of these films was obtained by Tauc method using the following equation:

$$(\alpha h\nu)^{\frac{1}{2}} = B(E_g - h\nu)$$

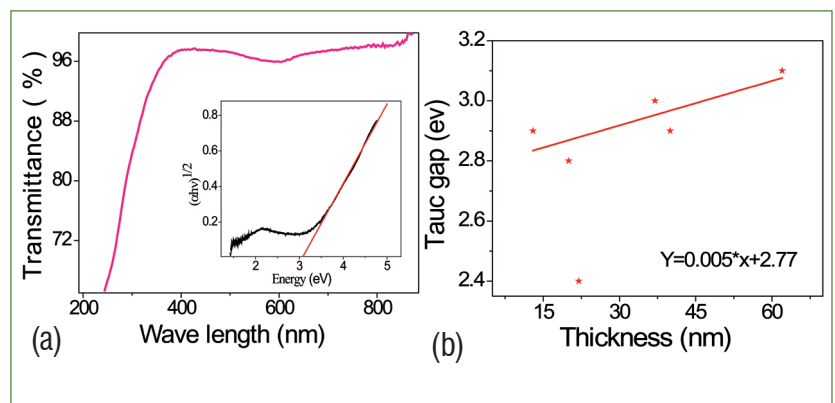


Figure 7: (a) UV-Vis transmittance vs energy plot of the DLC film and (b) the variation of band gap with respect to nominal thickness

where α is the absorption co-efficient, h is the Planck's constant, ν is the frequency of the incident photon and B is a constant. The calculated Tauc band gap of these films varied from 2.4 to 3.1 eV. The observed high band gap and high optical transparency are the inherent features of the diamond-like carbon films with higher sp³ content. Figure 7b shows the variation of band gap with nominal thickness of the films deposited on Si substrate. As shown in the figure, the Tauc gap increases with thickness suggesting higher sp³ bonding in thicker films.

Ultra smooth and uniform diamond-like carbon films are successfully synthesized by ECR-CVD and the properties have been studied with respect to methane concentration and microwave energy. It is found that the change in methane concentration leads to a significant variation in growth rate. On the other hand, the increase in microwave energy greatly influences the source ion flux density, as well as the chemical bonding of the films and hence increases the density of the films. The thickness of these films is in the range of 13 to 62 nm and rms roughness of the films is constant about 2.4 \AA irrespective of thickness. The Raman analysis confirmed that the films contains higher sp³ fraction and it increases with the film thickness. The hydrogen content increased with film thickness and it stabilizes the sp³ bonding consequently Tauc gap also increases but the film density reduces. These results suggest that the film growth mechanism is controlled by a sub-implantation process. In conclusion, the ECR-CVD technique has proved to have an immense control over the structural as well as optical properties of the diamond-like carbon films. Thus, the improved thin diamond-like carbon films can be effectively used in various fields including protective coatings, electronic and mechanical applications.

Reported by Syamala Rao Polaki
Surface & Nanoscience Division
Materials Science Group

Young Researcher's FORUM

Thermodynamics and Kinetics of Phase Transformation in Ti-Ta-Nb Alloy

Titanium and its alloys are widely used as structural material in various industries like aerospace, chemical, petrochemical, nuclear and biomedical industries owing to their high strength to weight ratio, superior corrosion resistance, lower elastic modulus and biocompatibility. In recent times, more attention is paid to the development of titanium alloys with β phase stabilizing elements such as Ta, Nb and Mo, because of their high strength, lower elastic modulus and non-toxic nature. These alloys find extensive applications in biomedical and nuclear industries. It is well known in alloy design that the properties of the alloy can be controlled by tailoring the microstructure. The innumerable microstructures exhibited by Ti alloys stem from the existence of the $\alpha \leftrightarrow \beta$ structural phase transformation. The phase transformation and the resultant microstructures are strongly influenced by the chemical composition of the alloy, heat and thermo-mechanical treatment. The nature of phase transformation is thus controlled by thermodynamic and kinetic parameters. It can be said that a prior knowledge of thermo-kinetic data of phase transformation is important in designing the alloy and optimising the processing route to meet the end application. In this article, the thermodynamics and kinetics of $\alpha \leftrightarrow \beta$ phase transformation in Ti- 5mass%Ta- 1.8mass%Nb alloy is discussed. This alloy has



Mrs. Madhusmita Behera did her Masters in Chemistry from Utkal University, Bhubaneswar, Odisha. She joined IGCAR as a DAE research fellow in Chemical Sciences in August 2007 and carried out her doctoral work in the Microscopy and Thermophysical Properties Division, PMG, under the guidance of Dr. Saroja Saibaba. She has submitted her doctoral thesis titled "A study on high temperature phase stability and phase transformation characteristics using calorimetry and microscopy techniques" to Homi Bhabha National Institute, Mumbai in November 2012 and has completed her viva-voce successfully in April 2013.

been developed indigenously as a candidate structural material for nuclear spent fuel reprocessing application in highly oxidizing and corrosive media, due to its excellent corrosion resistance, as compared to pure Ti and stainless steel. It has also been used as the filler material for the welds in Ti dissolvers fabricated in IGCAR, for the above reasons.

The alloy was melted by a triple vacuum arc remelting method at NFC, Hyderabad. The as-cast alloy was subjected to a series of thermomechanical processing steps and received in the form of rods. The alloy was further stress relieved in the $\alpha + \beta$ phase field by holding for 5 hours at 973 K and used as the starting material for the present study. The structure and microstructure were characterized by X-ray diffraction and both conventional and electron microscopy. The XRD pattern reveals the presence of the major α -hcp phase and the room temperature microstructure consists of fine equiaxed α grains (Figure 1 and 2). The phase transformations that occur in the solid state represent the thermodynamic instabilities of different phases. While the stability of different phases is decided by the thermodynamic properties, it is the kinetics of the phase transformations that dictates the rate at which the transformation attains the true thermodynamic equilibrium. Hence, in this study the thermodynamic properties of the alloy were measured using

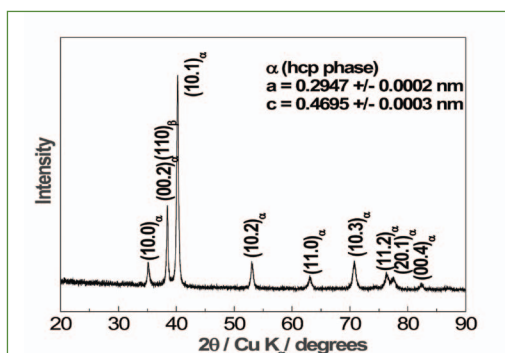


Figure 1: The room temperature XRD pattern of the Ti- 5mass%Ta- 1.8 mass%Nb alloy showing the presence of α - phase

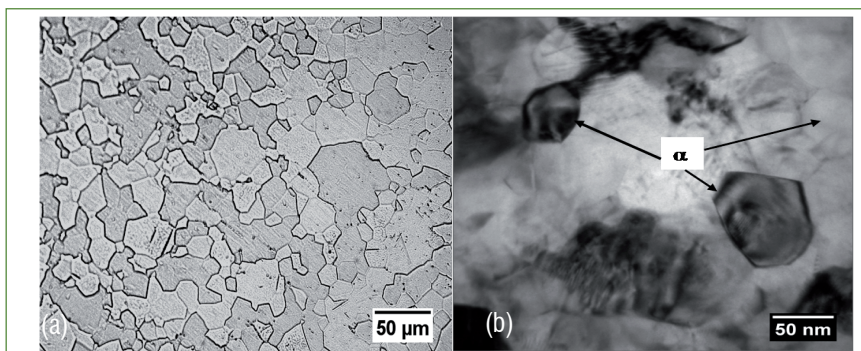


Figure 2: (a) Optical and (b) TEM micrograph showing fine equiaxed grains of α - phase

inverse drop calorimetry and differential scanning calorimetry has been used to study the kinetics of phase transformation.

Thermodynamic Properties

Enthalpy Increment ($H_T - H_{298.15}$) variation with temperature

The enthalpy increment ($H_T - H_{298.15}$) was measured as a function of temperature in the range of 463-1457 K using inverse drop calorimetry. The data points represent the measured enthalpy and the line joining them serves to delineate the observed temperature dependence of the enthalpy variation. It is observed from Figure 3, that the enthalpy increment ($H_T - H_{298.15}$) for the low temperature α -phase increases steadily in a non-linear fashion with temperature up to about 1072 K. At this temperature there is a clear change in the enthalpy variation behaviour indicating the possible commencement of $\alpha \rightarrow \beta$ phase transformation. In $\alpha \rightarrow \beta$ transformation region, the enthalpy increment values show a steeply rising character with temperature. This trend persists until about 1156 K and subsequently, another marked change in the enthalpy variation has been observed. This second inflection temperature corresponds to completion (T_f) of β -phase formation. Accordingly, 1072 ± 2 K and 1156 ± 2 K are taken as the start (T_s) and finish (T_f) of $\alpha \rightarrow \beta$ diffusional phase transformation for Ti- 5Ta- 1.8Nb alloy. In the β -phase regime, the enthalpy again shows a continuous, non-linear increase with temperature.

Analytical representation of enthalpy increment ($H_T - H_{298.15}$) data

In the present study, the variation of experimental enthalpy increment with temperature in the range 463-1457 K is non-linear and exhibits a discontinuous change associated with $\alpha \rightarrow \beta$ phase transformation. Hence, the enthalpy increment data in α , $\alpha + \beta$ and β phase regions are fitted to the following expressions and the corresponding specific heat (C_p) values are calculated from these fit expressions.

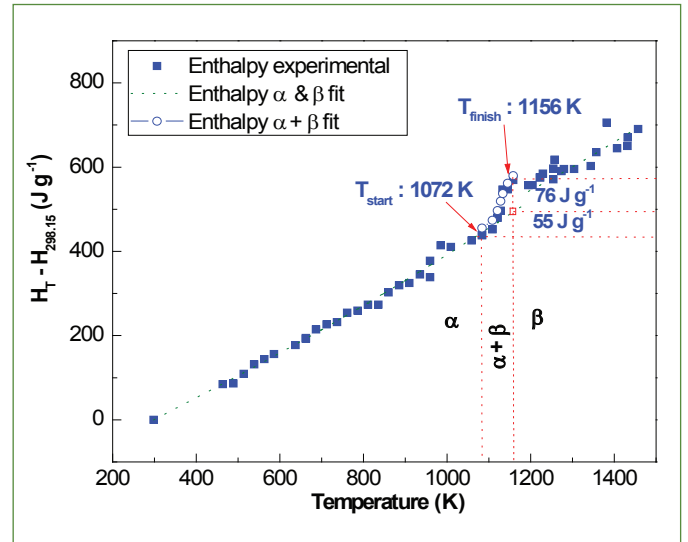


Figure 3: Variation of enthalpy increment with temperature for Ti- 5mass%Ta- 1.8mass%Nb alloy

α phase: $463 \text{ K} \leq T \leq 1072 \text{ K}$

The enthalpy increment data in α phase ($463 \text{ K} \leq T \leq 1072 \text{ K}$) are fitted by non-linear least square regression method to the following expression is given as equation 1 in Table 1.

The equation 1 for α phase domain is chosen by fixing $\Delta^0 H_{298.15} = 0$ and the specific heat C_p at 298.15 K is $519 \text{ J kg}^{-1} \text{ K}^{-1}$. The specific heat value in the same range is reported for Ti-4Nb-4Zr alloy. The specific heat in α phase domain derived by taking the derivative of the equation 1, is given in equation 2.

$\alpha \rightarrow \beta$ transformation region: $1072 \text{ K} \leq T \leq 1156 \text{ K}$

Unlike in a unary system, the phase transformation in an alloy occurs over a range of temperatures. Hence, in the $\alpha \rightarrow \beta$ transformation region both the α and β phases coexist in finite

Table 1: Equations

$\Delta^0 H / \text{J g}^{-1} = [H_T - H_{298.15}] = 0.39964 (T - 298.15) + 1.1 \times 10^{-4} (T^2 - 298.15^2) - 4.825 \times 10^3 (T^{-1} - 298.15^{-1}) \quad (1)$	$\Delta^0 H_T / \text{J g}^{-1} = 0.22515 T + 1.5 \times 10^{-4} T^2 + 7.0534 \times 10^4 T^{-1} \quad (7)$
$C_p / \text{J kg}^{-1} \text{ K}^{-1} = d(\Delta^0 H) / dT = 399.64 + 0.22 T + 4.825 \times 10^6 T^{-2} \quad (2)$	$C_p / \text{J kg}^{-1} \text{ K}^{-1} = d(\Delta^0 H_T) / dT = 225.15 + 0.3 T - 7.0534 \times 10^7 T^{-2} \quad (8)$
$\Delta^0 H_T = [f_\alpha \Delta^0 H_T^\alpha + f_\beta \Delta^0 H_T^\beta] + \Delta^0 H_{tr} \quad (3)$	$f(T) = \int_{T_s}^T y(T) dT / \int_{T_s}^{T_f} y(T) dT \quad (9)$
$\Delta^0 H_T / \text{J g}^{-1} = [H_T - H_{298.15}] = \{0.39964 (T - 298.15) + 1.1 \times 10^{-4} (T^2 - 298.15^2) - 4.825 \times 10^3 (T^{-1} - 298.15^{-1})\} + f_\beta(T) \Delta^0 H_{tr} \quad (4)$	$f(T) = 1 - \exp\{-k^n [R(T - T_s)^2 / \phi Q_{eff}^n]\} \quad (10)$
$f_\beta(T) = 1 - \exp\{-k_0^n \exp\{(-nQ_{eff}/RT)\} (R(T - T_s)^2 / \phi Q_{eff}^n)\} \quad (5)$	$k = k_0 \exp(-Q_{eff} / RT) \quad (11)$
$\Delta C_p^{\alpha \rightarrow \beta} / \text{J kg}^{-1} \text{ K}^{-1} = 399.64 + 0.22 T + 4.825 \times 10^6 T^{-2} + f_\beta \Delta^0 C_p + df_\beta / dT (\Delta^0 H_{tr}) \quad (6)$	$f(T) = 1 - \exp\{-k_0^n \exp\{(-nQ_{eff}/RT)\} (R(T - T_s)^2 / \phi Q_{eff}^n)\} \quad (12)$

amount and the amount of α phase continuously changes with temperature until it completely transforms to β . Hence, the total enthalpy increment ($\Delta^{\circ}H_T$) at any temperature T in the $\alpha+\beta$ two phase domain is basically a sum of two independent contributions. Of these, the first one comes from the weighted sum of individual enthalpy contributions from α and β phases. The other one, termed as the phase transformation enthalpy ($\Delta^{\circ}H_{tr}$) arises from the so-called latent heat associated with $\alpha \rightarrow \beta$ phase transformation. Thus to a first approximation the total measured enthalpy increment $\Delta^{\circ}H_T$ in the transformation domain ($1072 \text{ K} \leq T \leq 1156 \text{ K}$) may be written as given in equation 3, where

$$f_{\alpha}(T) + f_{\beta}(T) = 1$$

$f_{\alpha}(T)$ and $f_{\beta}(T)$ denote the fraction of α and β phases respectively present at temperature T , $\Delta^{\circ}H_T^{\alpha}$ and $\Delta^{\circ}H_T^{\beta}$ are the enthalpy increment of α and β phases respectively at temperature T . The latent heat or the enthalpy for the $\alpha \rightarrow \beta$ phase transformation ($\Delta^{\circ}H_{tr}$) for the alloy is determined by using equation 3 and it is possible only when $\Delta^{\circ}H_T^{\alpha}$, $\Delta^{\circ}H_T^{\beta}$, f_{α} and f_{β} are known as explicit functions of temperature. It can also be said that the individual enthalpy contributions from α and β phases cannot be estimated *a priori* in the transformation region. In such a situation, the values for $\Delta^{\circ}H_T^{\alpha}$ and $\Delta^{\circ}H_T^{\beta}$ in the phase transformation domain have to be obtained only as extrapolations of their respective trends in the corresponding low temperature α and high temperature β phase region. This procedure is illustrated in Figure 3, where the dotted line emanating from T_s indicates the enthalpy behaviour of α phase into the transformation domain and is taken to be valid up to T_f . In the second step at T_f , the $\alpha \rightarrow \beta$ transformation is allowed to take place isothermally till it reaches completion and the enthalpy involved in this step gives the enthalpy for $\alpha \rightarrow \beta$ transformation ($\Delta^{\circ}H_{tr}$). It can also be seen from the figure that the total increase in enthalpy in the $\alpha \rightarrow \beta$ transformation domain ($1072 \text{ K} \leq T \leq 1156 \text{ K}$) is $131 \pm 12 \text{ J g}^{-1}$. The entire quantum of this 131 J g^{-1} could not contribute to the enthalpy change associated with $\alpha \rightarrow \beta$ transformation. It includes both the enthalpy contribution from α and β phases and the transformation enthalpy which can be mathematically represented by equation 3. Hence, the $\alpha \rightarrow \beta$ transformation enthalpy ($\Delta^{\circ}H_{tr}$) calculated by the extrapolation method for Ti- 5 mass%Ta - 1.8 mass% Nb alloy is 76 J g^{-1} and the contribution from α and β phases is 55 J g^{-1} which corresponds to the first term inside the square braces on right side of equation 3 and graphically shown in Figure 3. Thus, in the final analysis, the total enthalpy increment ($\Delta^{\circ}H_T$) in the transformation zone is represented by the following expression as given in equation 4.

It is reiterated here that the first term inside the curved braces on the right hand side of equation 4 denotes the α -phase enthalpy which is extrapolated up to T_f . The second term is the transformation component.

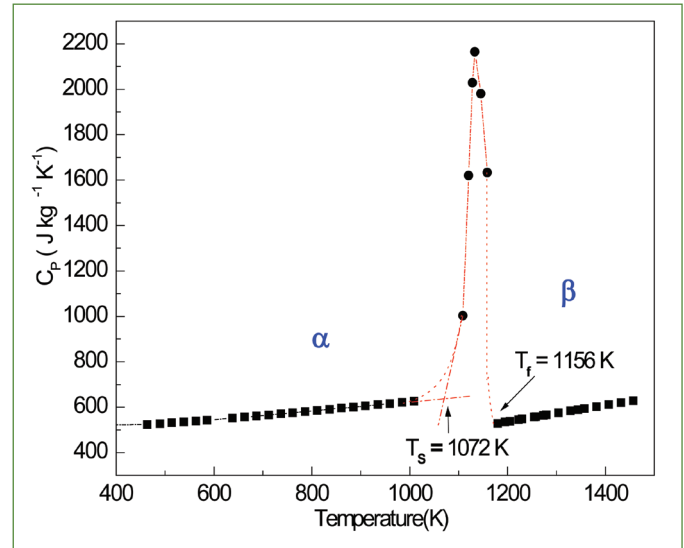


Figure 4: Variation of specific heat C_p with temperature

The temperature dependent experimental enthalpy data corresponding to the transformation temperature zone which represents the progress of $\alpha \rightarrow \beta$ transformation are fitted to an empirical model for the diffusional phase transformation kinetics name by the Kolmogorov-Johnson-Mehl-Avrami (KJMA) model. According to this model, $f_{\beta}(T)$ is given by the following expression as given in equation 5.

Here, Q_{eff} represents the apparent activation energy for the overall transformation, n is an empirical transformation exponent, k_0 is the frequency factor, R is the universal gas constant and ϕ corresponds to slow rates of heating such that at each temperature T in the transformation zone, the equilibrium limit of $f_{\beta}(T)$ is realised. The following values of the kinetic quantities: $n = 1.1$; $Q_{eff} = 295 \text{ kJ mol}^{-1}$; and $k_0 = 1.06 \times 10^{13} \text{ s}^{-1}$ are obtained for $\alpha \rightarrow \beta$ transformation in Ti- 5mass%Ta- 1.8mass%Nb alloy. Substituting equation 5 in equation 4 the enthalpy in the transformation domain can be generated. The specific heat C_p expression in the transformation zone is obtained by taking the derivative of equation 4 with respect to T is given in equation 6.

Here, $\Delta^{\circ}C_p$ is the change in C_p associated with $\alpha \rightarrow \beta$ phase transformation. Its value is estimated to be $(\Delta^{\circ}H_{tr}/\Delta T) = 904 \text{ J Kg}^{-1} \text{ K}^{-1}$.

β phase: $1156 \text{ K} \leq T \leq 1457 \text{ K}$

In the β -phase region the enthalpy increment values are fitted to the following expression and is given in equation 7.

The specific heat C_p in the β -phase can be represented by the following expression as given in equation 8.

The variation of C_p with temperature in α -phase, in the $\alpha \rightarrow \beta$ phase transformation region and in β - region are shown in Figure 4.

Kinetics of $\alpha \leftrightarrow \beta$ Phase Transformation

Effect of heating and cooling rate on transformation arrest temperatures (T_s , T_p , T_f)

The kinetics of $\alpha \leftrightarrow \beta$ phase transformation in Ti-5Ta-1.8Nb alloy has been studied using differential scanning calorimetry. The DSC experiment was performed by heating the sample at a fixed rate (ϕ_h) from 473.15 to 1273.15 K (β -bcc phase) followed by equilibration at this temperature for about 15 minutes and cooled to room temperature at a fixed rate (ϕ_c), employing scanning rates between 3 and 99 K min⁻¹. The on-heating and cooling DSC profile obtained at a scan rate of 20 K min⁻¹ is shown in Figure 5.

The presence of clear and reasonably sharp endothermic and exothermic peaks during heating and cooling in Figure 5 are indications of the occurrence of diffusional $\alpha \rightarrow \beta$ and $\beta \rightarrow \alpha$ phase transformations respectively. The start (T_s) and finish (T_f) temperatures of $\alpha \leftrightarrow \beta$ transformation are clearly delineated from Figure 5. The transformation arrest temperatures (T_s , T_p , T_f) during heating and cooling as a function of scan rates are shown in Figure 6. It is observed from Figure 6 that there is a general increase (or decrease) in transformation arrest (T_s , T_p , T_f) temperatures with increase in heating (or cooling) rates and this increase (or decrease) in transformation arrest temperatures are nonlinear in nature. This nonlinearity with heating rate is quite significant for transformation peak (T_p) and finish temperatures (T_f), whereas the transformation start temperature (T_s) attains saturation at higher heating rates (ϕ_h) after an initial increase at low heating rate. As a result, the width of the transformation domain ($\Delta T_{tr} = T_f - T_s$) increases which implies kinetics induced expansion of ($\alpha + \beta$) two phase fields for high heating or cooling rates. This dependency of transformation arrest temperatures on the heating and cooling rate is inherent to the various nucleation and growth

mechanism through which the transformations progress. This can be explained based on the minimum time called incubation time needed for the nucleation of any phase at any temperature higher than the equilibrium transformation temperature. Hence, by the time the system completes its incubation; its temperature is either increased or decreased by the scanning heating or cooling rates respectively. It has also been observed from Figure 6 that there is considerable degree of under cooling during $\beta \rightarrow \alpha$ transformation. This undercooling effect increases with increase in cooling rate.

Fraction transformed and transformation kinetics

It is known that both $\alpha \rightarrow \beta$ and $\beta \rightarrow \alpha$ transformations are diffusive in nature for the entire range of heating and cooling rates (3-99 K min⁻¹). As it is well known that the degree of transformation is equal to the fraction of heat absorbed or released, hence the fractional extent of transformation $f(T)$ as a function of temperature is calculated from the experimental DSC profile using the following expression as given in equation 9. $y(T)$ is the baseline compensated heat flux signal, measured as a function of T , in the range, $T_s \leq T \leq T_f$. Here, the integral in the numerator stands for the partial area under the peak in the temperature domain T_s - T and the denominator stands for the total peak area covering the entire transformation temperature range (T_s - T_f). The estimation of degree of transformation as a function of temperature using equation 9 is done by assuming that the transformation is 100% complete upon reaching T_f . But this is generally not the case, especially in case of higher scan rates due to the kinetic lag. The fraction of β and α phase formed as a function of temperature during heating and cooling using equation 9 are shown in Figures 7a and b respectively. The fraction transformed curves show sigmoidal behavior for the entire range of heating and cooling

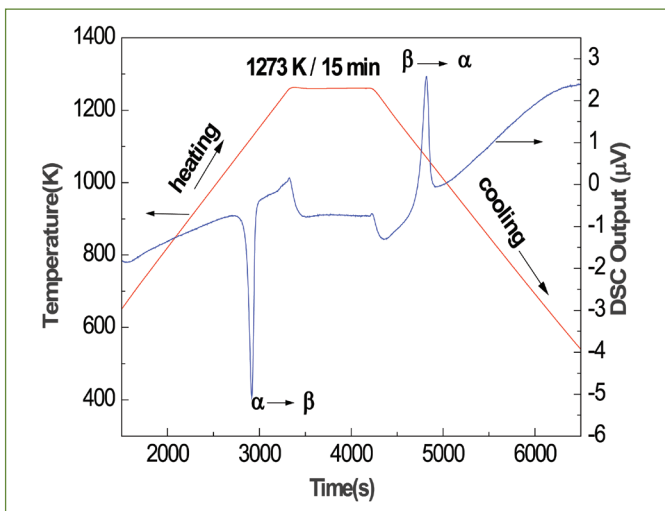


Figure 5: DSC profile at a heating and cooling rate of 20 K min⁻¹

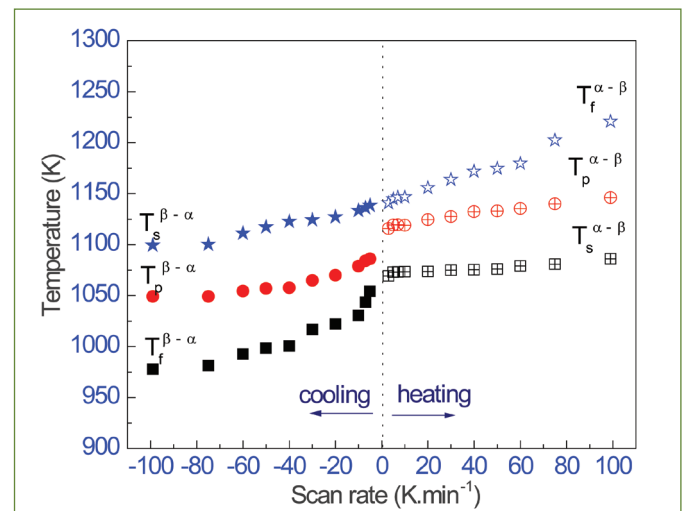


Figure 6: Graphical representations of heating and cooling rate variation of transformation start (T_s), peak (T_p) and finish (T_f) temperatures

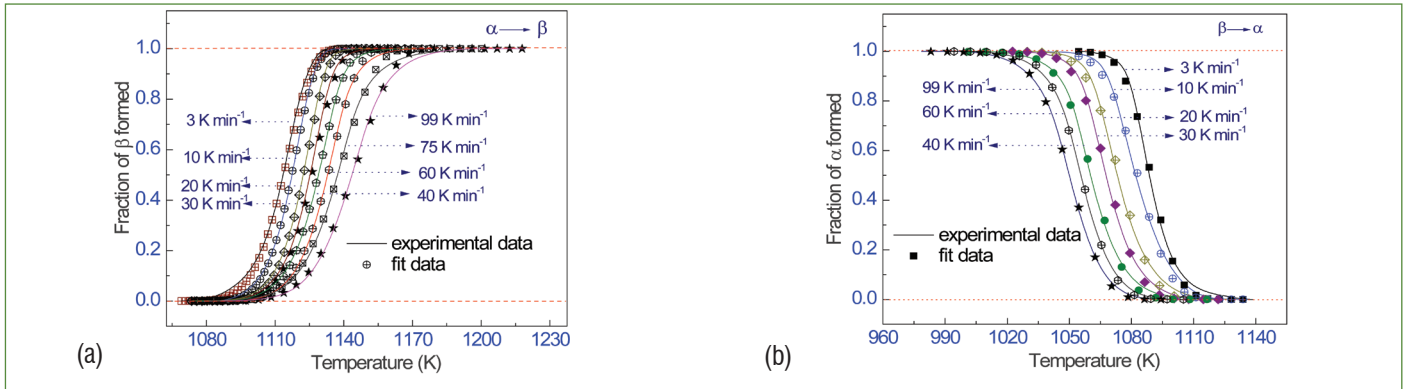


Figure 7: Experimentally obtained transformation plot for (a) $\alpha \rightarrow \beta$ transformation, (b) $\beta \rightarrow \alpha$ transformation. The line represents the experimental data, while the symbols are the non-isothermal KJMA fit

rates of the present study, which confirms the diffusion mediated nucleation and growth based transformation. In this alloy the $\alpha \leftrightarrow \beta$ transformation takes place by the diffusion of Ta and Nb in the Ti matrix. Hence, the experimental data on fraction transformed $f(T)$ for $\alpha \leftrightarrow \beta$ transformation are fitted to the following non-isothermal version of KJMA model under site saturation condition which is given by the following expression as equations 10 and 11. Hence, the above equation 10 can be written as equation 12. Where, Q_{eff} is the overall (both nucleation and growth) activation energy, k_0 = pre exponential factor, n = the Avrami (growth) exponent which gives an indication about the mechanism and the dimensionality of growth of product phase. The fitting of fraction transformed curve is done by a standard non-linear optimization method. The resulting values for the kinetic quantities Q_{eff} , n , k_0 for both $\alpha \rightarrow \beta$ and $\beta \rightarrow \alpha$ transformation are listed in Table 1. It can be seen from the table that Q_{eff} , the effective activation energy is in the range of 280-290 kJ mol^{-1} for $\alpha \rightarrow \beta$ phase transformation,

where as for $\beta \rightarrow \alpha$ phase transformation it varies between 80-110 kJ mol^{-1} . The Avrami (growth) exponent (n) varies between 1.18-1.95 during $\alpha \rightarrow \beta$ transformation and assumes a higher value of nearly 3 during $\beta \rightarrow \alpha$ transformation. The high value of Q_{eff} obtained for $\alpha \rightarrow \beta$ phase transformation is attributed to the volume diffusion of Ta and Nb in the Ti matrix. The low value for the transformation exponent for $\alpha \rightarrow \beta$ phase transformation is due to the growth impingement effects strongly operating under site-saturation nucleation conditions. The low value of activation energy obtained for $\beta \rightarrow \alpha$ phase transformation may be possibly due to availability of short circuit paths in addition to volume diffusion.

*Reported by Madhusmitha Behera
Microscopy and Thermophysical Properties Division
Physical Metallurgy Group, MMG*

Table 1: The resulting values for the kinetic quantities Q_{eff} , n , k_0 for both $\alpha \rightarrow \beta$ and $\beta \rightarrow \alpha$ transformation

ϕ (K min^{-1})	n	Q_{eff} (kJ mol^{-1})	$k_0 \times 10^{13}$ (s^{-1})	R^2	n	Q_{eff} (kJ mol^{-1})	$k_0 \times 10^4$ (s^{-1})	R^2
$\alpha \rightarrow \beta$ transformation (heating)					$\beta \rightarrow \alpha$ transformation (cooling)			
3	1.51	290	1.81	0.99	2.22	81	0.119	0.99
7	1.69	278	1.85	0.99	3.33	91	0.856	0.99
10	1.79	280	2.93	0.99	3.63	95	2.28	0.99
20	1.91	284	6.74	0.99	3.8	98	7.20	0.99
30	1.82	281	6.74	0.99	3.99	90	3.84	0.99
40	1.72	283	8.05	0.99	3.99	100	17.0	0.99
50	1.70	282	8.65	0.99	3.9	106	50.69	0.99
60	1.65	281	8.75	0.99	3.72	106	61.0	0.99
75	1.38	282	8.93	0.99	3.61	102	53.7	0.99
99	1.32	281	8.94	0.99	3.4	108	140.0	0.99

Conference and Meeting Highlights

Technology Day Celebrations 2013

May 11, 2013



Dr. P. Sivakumar, Director, CVRDE, DRDO, Chief Guest delivering the inaugural address during the inaugural session

IGCAR organized the “National Technology Day” celebrations on **May 11, 2013** at Convention Centre, Anupuram. This trilingual seminar (English, Hindi and Tamil) had participation from non-gazetted staff belonging to the various groups, accounts and administration. The technical meet comprised oral and poster presentations as well as display of component / product / devices / models developed by the participants. In total, 57 oral presentations, 111 poster presentations and 23 exhibits were presented by the participants show-casing their contribution, capability, knowledge and technical skill.

The programme started with the inaugural session with Dr. P. Sivakumar, Director, CVRDE, DRDO, Chennai as the Chief Guest. Dr. P.R. Vasudeva Rao, Director, IGCAR presided over the function and briefed the gathering about the genesis of the Technology Day Meet 2013. He reiterated that the objective of this event was to recognize and show-case the technical accomplishments of IGCAR personnel that had played a significant role in the success of the FBR programme. On behalf of Shri G. Srinivasan, Chairman, Organising Committee, Shri P.V. Kumar, Project Director, FRFCF highlighted the significance of the National Technology Day and its importance to the gathering. In his inaugural address and technical presentation, Dr. P. Sivakumar brought out the great strides made by the technical and scientific organizations of our country with specific emphasis on the progress made by the Defence sector.

He graphically demonstrated these facts with a very impressive audio visual display highlighting the significant contributions made by the Defence Research and Development Organization (DRDO) of India. He also emphasized the need for the R&D organizations of our country to contribute towards social responsibilities which included but are not limited to providing clean drinking water, energy and better education to the people of our nation at large. Dr. U. Kamachi Mudali, Secretary welcomed the gathering and Dr. K. Ananthasivan, Convenor, proposed the vote of thanks.

Subsequently, four parallel technical sessions comprising oral presentations were conducted at the Convention Centre and SRI Guest House Seminar Hall. Technical posters and exhibits were displayed at the Convention Centre. A total of 202 non-gazetted staff from IGCAR participated with great zeal and enthusiasm and displayed their technical skills and contributions with pride.

In the concluding session, Dr. P.R. Vasudeva Rao, Director, IGCAR appreciated the spirit and enthusiasm shown by the participants in showcasing their excellent contributions that form a significant part of the collective achievements of IGCAR. Participation certificates were given by Director, IGCAR to all the participants.

*Reported by U. Kamachi Mudali
Secretary,
Technology Day Celebrations 2013*

News & Events

SAFETY PROMOTIONAL ACTIVITIES

In order to fulfill safety, health and environment requirements and promote positive safety culture at the workplace, safety promotional activities such as Fire Service Week and World Environment Day are being organized by Environment and Safety Division of IGCAR every year.

Fire Service Week

April 14, 2013 is observed as Fire Service Day in memory of brave firemen who laid down their lives in fighting the fire that broke out due to a huge explosion from a ship loaded with 1200 tons of explosives, cotton bales and oil drums at Victoria Dockyard, Mumbai. The explosion resulted in huge loss of life and property. Since then April 14-20, has been observed as National Fire Service Week. At IGCAR the same was observed on **April 17, 2013**. On this occasion, an invited talk on 'Risk Assessment' was delivered by Shri R.M. Kshirsagar, Senior Manager (Fire & Safety), Chennai Petroleum Corporation Limited, Chennai. Live demonstrations of Fire Fighting Equipment was arranged for our employees with the help of M/s. Safex Fire Services Limited, Chennai. To inculcate fire safety culture among employees, competitions such as essay, poster and slogan were conducted. Prizes were distributed to the winners by Shri S.A.V. Satyamurty, Director, EIRSG.



Shri S.A.V. Satyamurty, Director, EIRSG giving away the prize to one of the winners



Dr. K.K. Satpathy, Dr. Ajay Parida, Shri R. Natarajan, Dr. Prabhat Kumar and Dr. B. Venkatraman during World Environment Day 2013 Celebrations at IGCAR

Director, M.S. Swaminathan Research Foundation (MSSRF), Chennai. Dr. Parida highlighted the need for conserving food for future generations with an emphasis on food security of the country and its challenges. Dr. M.V.R. Prasad, Head, Environmental & Occupational Health Section proposed the vote of thanks. About 250 employees participated in the function. About thirty saplings were planted on the new road near FRFCF by the dignitaries.

World Environment Day

World Environment Day (WED) is observed all over the world on 5th of June every year. The same was celebrated at IGCAR on **June 5, 2013** at Sarabhai auditorium. Dr. K.K. Satpathy, Head, Environment & Safety Division (EnSD), IGCAR delivered the welcome address. Dr. Prabhat Kumar, Chairman and Managing Director (CMD), BHAVINI, inaugurated the programme and delivered the inaugural address. Shri R. Natarajan, Director, RpG and ESG (M&E) delivered the presidential address. An invited talk on "Challenges for feeding a billion plus" was delivered by Dr. Ajay Parida, Executive

Forthcoming Meeting and Conference

International Conference on Structural Integrity (ICONS-2014)

The first International Conference on Structural Integrity (ICONS-2014) is being organized in Kalpakkam during February 4-7, 2014 by IGCAR in collaboration with Society for Failure Analysis (SFA) - Chennai Center, Indian Institute of Metals (IIM) - Kalpakkam Chapter, and Indian Institute of Welding (IIW) - Chennai Branch. International experts will give keynote and invited talks in structured technical sessions and delegates from R&D, academic institutes and industry will take part in ICONS-2014 to share the state-of-the-art advances in various aspects of structural integrity including the following:

- Advanced structural materials
- Corrosion and coatings
- Creep and creep-fatigue
- Design and stress analysis
- Fabrication technology and CAM
- Failure analysis and damage mechanics
- Fatigue and fracture mechanics
- Hard facing and tribology
- ISI, remote handling and robotics
- Life prediction and life extension
- Mechanical property evaluation
- Metal joining and welding
- Microstructure characterization
- Nondestructive evaluation and QA
- Numerical modeling and validation
- Reliability and regulatory aspects
- Structural health monitoring and condition monitoring

Address for correspondence

Dr. T. Jayakumar

Chairman, Organising Committee, ICONS-2014

Distinguished Scientist & Director, Metallurgy and Materials Group

Indira Gandhi Centre for Atomic Research (IGCAR)

Kalpakkam - 603102 (Tamil Nadu), INDIA

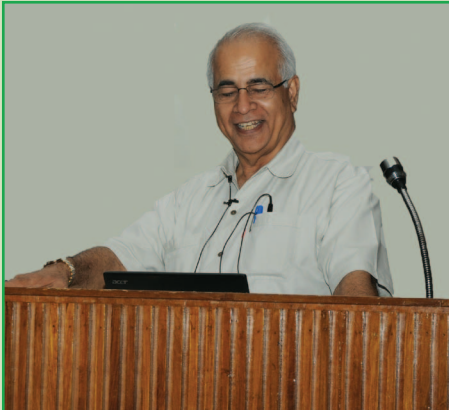
Phone: 044-27480107 / 27480232

E-mail: icons2014@igcar.gov.in

Fax: 044-27480075 / 27480356

Webpage: <http://icons2014.com/>

Visit of Dignitaries



Dr. Jatinder V. Yakhmi, Chairman, Atomic Energy Education Society (DAE), Advisor to the Chairman, AEC and Raja Ramanna Fellow, Homi Bhabha National Institute, Mumbai, delivered the IGC Colloquium on "Matter and Materials: Soft and Nano, Naturally", during his visit to the Centre on **April 12, 2013**.

Dr. Jatinder V. Yakhmi, Chairman, Atomic Energy Education Society, DAE delivering the IGC Colloquium on "Matter and Materials: Soft and Nano, Naturally" during his visit to the Centre

Delegation of Editors/Senior Journalists from Nepal visited the Centre on **April 25, 2013**. During the meeting with Shri R. Natarajan, Director, RpG and ESG (M&E), they were briefed about "Fast Reactors for Energy Security" by Dr. M. Sai Baba, Associate Director, Resources Management Group, followed by presentation on "Plant Overview" by Shri V. G. Mohan Nayar, Training Superintendent, Nuclear Training Centre, NPCIL. After the meeting the delegation visited the Madras Atomic Power Station.



Delegation of Editors/Senior Journalists from Nepal with Shri R. Natarajan, Director, RpG and ESG (M&E) and senior colleagues of the Department



Dr. Srikumar Banerjee, DAE Homi Bhabha Chair Professor & Former Chairman, AEC, during his visit to the Centre on **June 3, 2013** delivered the IGC Colloquium on "Evolving Nuclear Fuel Cycle".

Dr. Srikumar Banerjee, DAE Homi Bhabha Chair Professor & Former Chairman, AEC, delivering the IGC Colloquium on "Evolving Nuclear Fuel Cycle" during his visit to the Centre

Awards & Honours

Dr. U. Kamachi Mudali has been elected as “Fellow of ASM” by the Board of Trustees of ASM International, USA for outstanding contribution in the development and application of corrosion-resistant advanced materials and coatings for critical uses in nuclear and related industries in 2013.

Dr. U. Kamachi Mudali is appointed as Member of Editorial Board of the Indian National Academy of Engineering, INAE, 2013.

Best Paper/Poster Award

Under Sodium Imaging of SFR Internals : Simulation Studies in Water

Dr. Anish Kumar, Shri G. K. Sharma, Dr. C. Babu Rao, Dr.B. Purnachandra Rao, Dr. T. Jayakumar from MMG
Shri G. Gobillot, Shri F. Le Bourdais from CEA, France

International Conference on Advancements in Nuclear Instrumentation Measurement Methods and their Applications (ANIMMA 2013), June 23-27, 2013, Marseille, France

Best Poster Paper Award

Experience in Fabrication of Stainless Steel Hoods for Glove Boxes for Handling Radioactive Materials

Shri Abhishek Kumar Yadav, Shri R. Lavakumar, Shri T.V. Prabhu and Shri G. Ravisankar from ROMG
Advances in Welding Science & Technology (ADWEST-2013), Puducherry, May 3-4, 2013
organized by Indian Institute of Welding

Third Best Presentation Prize

Self Healing Corrosion Resistant Coatings Based on Inhibitor Loaded TiO₂ Nanocontainers

Shri C. Arunchandran, Dr. S. Ramya, Dr. R. P. George, Dr. U. Kamachi Mudali from MMG
Journal of the Electrochemical Society (JES) 159 (11) (2012) pp. C552-C559.

IIM Young Researcher Best Paper Award

Manifestation of Dynamic Strain Aging (DSA) during Elevated Temperature Ratcheting of type 316LN Stainless Steel

Shri Aritra Sarkar, Dr. A. Nagesha, Dr. R. Sandhya and Dr. M.D. Mathew from MMG
International conference and exhibition of pressure vessels and piping (OPE-2013)

Second Best Paper Award

Precipitation-hardening of Ni-based Superalloy 693

Shri A. Sarkar from MMG and Shri R. S. Dutta, Dr.R. Tewari and Dr. G. K. Dey from BARC
National Symposium on Materials and Processing (MAP-2012)

Best Poster Paper Award in Metal and Materials Category

Interaction of U³⁺ with O²⁻ in Molten LiCl-KCl Eutectic

Shri Suddhasattwa Ghosh, Smt. S.Vandarkuzhali, Shri S.Nedumaran, Dr. B. Prabhakara Reddy and
Dr. K.Nagarajan from CG

Conference on Molten Salts in Nuclear Technology (CMSNT-2013), Bhabha Atomic Research Centre,
Jan 9-11, 2013

Best Poster Award



Brown-headed Gulls

These were captured in the back waters of Kalpakkam

Dr. M. Sai Baba,

Chairman, Editorial Committee, IGC Newsletter

Editorial Committee Members: Dr. K. Ananthasivan, Shri M.S. Chandrasekar, Dr. N.V. Chandra Shekar, Dr. C. Mallika, Shri K. S. Narayanan, Shri V. Rajendran, Dr. Saroja Saibaba and Dr. Vidya Sundararajan